A searchable database and mass spectral comparison tool for aerosol mass spectrometry (AMS) and aerosol chemical speciation monitor (ACSM)

Sohyeon Jeon[1], Michael J. Walker[1], Donna T. Sueper[2,3], Douglas A. Day[2], Anne V. Handschy[2], Jose L. Jimenez[2], Brent J. Williams[1]

[1]Department of Energy, Environmental and Chemical Engineering, Washington University in St. Louis, St. Louis, MO, USA

[2]Department of Chemistry, and Cooperative Institute for Research in Environmental Sciences (CIRES), University of Colorado, Boulder, CO, USA

[3]Aerodyne Research Inc, Billerica, MA

Correspondence to: Brent J. Williams (brentw@wustl.edu)

Abstract. The Aerodyne Aerosol Mass Spectrometer (AMS) and Aerosol Chemical Speciation Monitor (ACSM) are the most widely applied tools for in-situ chemical analysis of the non-refractory bulk composition of fine atmospheric particles. The mass spectra (MS) of many AMS and ACSM observations from field and laboratory studies have been reported in peer-reviewed literature and many of these MS have been submitted to an open-access website. With the increased reporting of such data sets, the database interface requires revisions to meet new demands and applications. One major limitation of the web-based database is the inability to automatically search the database and compare previous MS with the researcher's own data. In this study, a searchable database tool for the AMS and ACSM mass spectral dataset was built to improve the efficiency of data analysis using Igor Pro, consistent with existing AMS and ACSM software. The database tool incorporates the published MS and sample information uploaded on the website. This tool allows the comparison of a target mass spectrum with the reference MS in the database, calculating cosine similarity, and provides a range of MS comparison plots, reweighting, and mass spectrum filtering options. The aim of this work is to help AMS users efficiently analyze their own data for possible source or atmospheric processing features by comparison to previous studies, enhancing information gained from past and current global research on atmospheric aerosol.

1. Introduction

Atmospheric aerosol particles have adverse effects on human health and impact visibility, the hydrological cycle, and climate changes through direct and indirect radiative properties (Ramanathan et al., 2001; Bäumer et al., 2008; Kampa and Castanas, 2008; IPCC, 2021). Globally, the dominant constituent of dry fine-mode respirable aerosol particles is organic matter (OM), commonly referred to as organic aerosol (OA). Understanding the characteristics, sources, and processes of OA is key in developing aerosol-related control policies and air quality and climate models. However, OA is chemically complex, with thousands of different compounds detected in single samples (Goldstein and Galbally, 2007). The compositional complexity of OA arises from diverse primary sources and reactions of organic species in the atmosphere that produce secondary OA (SOA) material from gas-to-particle conversion or chemically aged OA (De Gouw and Jimenez, 2009).

Aerosol Mass Spectrometry (AMS) has widely been applied to atmospheric science research for analysis of the bulk chemical composition of fine particles. It allows one to measure the non-refractory components of the particles with high time resolution, most typically reporting mass concentrations of total fine OA, sulfate, nitrate, ammonium, and chloride (e.g. Jayne et al., 2000; Jimenez et al., 2003; Allan et al., 2004; DeCarlo et al., 2006; Canagaratna et al., 2007; Baltensperger et al., 2010). The AMS has frequently been used in both field and laboratory studies. In field studies, the AMS has characterized atmospheric particles in environments such as urban, rural, remote, forested, ocean, and agricultural regions (e.g. Allan et al., 2004, 2006; Phinney et al., 2006; Aiken et al., 2009; He et al., 2011; Bates et al., 2012; Cleveland et al., 2012; Dall'Osto et al., 2013; Hao et al., 2014; Xu et al., 2014; Lee et al., 2015; Modini et al., 2015; Xu et al., 2015; Young et al., 2016; Kim et al., 2017). In addition, AMS has been used on many platforms such as mobile labs, aircraft, and ships as well as stationary sites (e.g. Bahreini

45 et al., 2003; Zorn et al., 2008; Mohr et al., 2011; Coggon et al., 2012; Drewnick et al., 2012; Claeys et al., 2017; Pirjola et al.,
46 2017; Robinson et al., 2018; Shilling et al., 2018). For laboratory studies, particles generated from a variety of sources,
47 including wood burning, cooking, trash burning, coal and fuel combustion, etc., have been characterized using AMS (e.g.
48 Canagaratna et al., 2004; Schneider et al., 2006; Aiken et al., 2008; Weimer et al., 2008; Mohr et al., 2009; Chirico et al., 2010;
49 He et al., 2010; Adam et al., 2011; Heringa et al., 2011; Wang et al., 2013; Collier et al., 2015; Fortenberry et al., 2018).
50 Furthermore, AMS has been employed to analyze SOA formed from different oxidation experiments using environmental
51 chambers or flow tube reactors with varying oxidants, aging processes, concentrations, humidity levels, temperatures,
52 precursors, etc. (e.g. Bahreini et al., 2005; Kroll et al., 2005, 2006; Murphy et al., 2007; Ng et al., 2007, 2008; Chhabra et al.,
53 2010; Lambe et al., 2011, 2012; Loza et al., 2014; Riva et al., 2016; Boyd et al., 2017; Lim et al., 2019).

54   The Aerosol chemical speciation monitor (ACSM) also has been used to analyze the bulk chemical composition of
55 non-refractory components with a very similar sampling and detection technology as the AMS. The key difference is that the
56 ACSM was developed with reduced complexity (e.g. no particle size measurement) and performance (Ng et al., 2011). A major
57 advantage of ACSM over AMS is that it provides a smaller size, lower cost, simpler operation, and less attention from site
58 managers than AMS. In addition, ACSM data are analyzed with the same techniques that are used for the AMS. Therefore, the
59 ACSM has been deployed for long-term monitoring at locations including urban (e.g. Ng et al., 2011; Sun et al., 2011;
60 Budisulistiorini et al., 2013; Carbone et al., 2013; Budisulistiorini et al., 2014; Aurela et al., 2015; Petit et al., 2015;
61 Budisulistiorini et al., 2016; Reyes-Villegas et al., 2016; Rattanavaraha et al., 2017; Sun et al., 2018; Kommula et al., 2021),
62 suburban (Zhang et al., 2018), rural (e.g. Tiitta et al., 2014; Canonaco et al., 2015; Fröhlich et al., 2015a; Parworth et al., 2015;
63 Bressi et al., 2016; Budisulistiorini et al., 2016; Schlag et al., 2016; Zhao et al., 2020), remote (e.g. Budisulistiorini et al., 2015;
64 Fröhlich et al., 2015b; Ripoll et al., 2015; Michoud et al., 2017), and forested areas (e.g. Fröhlich et al., 2013; Minguillón et
65 al., 2015; Heikkinen et al., 2020).

66   According to the broad and diverse application of the AMS and ACSM, data analysis procedures have also been
67 advanced to improve efficiency and accuracy to interpret the data. These advances have made it possible to divide the quantified
68 OA mass concentrations obtained from AMS and ACSM into hydrocarbon-like OA (HOA, a surrogate for primary OA (POA)
69 directly emitted from fossil fuel combustion) and oxygenated OA (OOA, a surrogate for SOA generated from a chemical
70 reaction or phase partitioning). Furthermore, OOA can be subdivided into low-volatility OOA (LV-OOA or more-oxidized
71 OOA, MO-OOA) and semi-volatile OOA (SV-OOA or less-oxidized OOA, LO-OOA) when combined with methods such as
72 thermal-denuding inlets and positive matrix factorization (PMF) analysis (Paatero and Tapper, 1994; Zhang et al., 2005; Lanz
73 et al., 2007; Ulbrich et al., 2009; Zhang et al., 2011). In addition, these deconvolved OA have been specifically characterized
74 depending on source types such as biomass burning (BBOA) and cooking (COA), increasing the utility of source apportionment
75 of atmospheric aerosols (Paatero and Tapper, 1994; Ulbrich et al., 2009; Mohr et al., 2009). This improvement in data analysis,
76 in addition to the higher performance and mass spectral resolution of modern time-of-flight (ToF) MS detectors often deployed
77 with the AMS and ACSM, has led to a growing number of reported measurements under various sample configurations and
78 conditions.

79   Mass spectra (MS) from the AMS and ACSM provide powerful information to interpret the OA data. A mass spectrum
80 with specific marker ions, or specific ratios of ions, can often be related to a source or chemical process. Here we broadly
81 classify MS types by mass resolution (unit mass resolution or UMR vs. high mass resolution or HR) and extent of MS separation
82 through data processing (non-deconvoluted/deconvoluted). UMR indicates that the signal at each mass is separated from the
83 next 'integer' m/z. In contrast, HR is able to quantify multiple HR ion fragments at a nominal m/z, which enables more detailed
84 characterization than UMR. DeCarlo et al., (2006) has demonstrated the ability to characterize HR ion fragments below a
85 nominal mass, typically m/z 120. These HR ion fragment signals can be grouped into different ion classes such as C_x, C_xH_y,
86 $C_xH_yO_z$, etc., which are called 'HR families'. A HR mass spectrum is often plotted in a color-coded stacked bar chart of these
87 HR families. Deconvolution indicates whether or not the MS are generated from an additional analysis step like PMF. If the
88 mass spectrum is obtained from PMF, it is called a 'Deconvoluted' mass spectrum and is identified as HOA, SV-OOA, LV-
89 OOA, etc. If not separated, the mass spectrum is referred to as 'Non-deconvoluted'. A non-deconvoluted MS may be
90 representative of multiple contributing sources or aging processes if an ambient sample or can be a single source or standard
91 observed in a lab study. Figure 1 presents various examples of AMS OA MS classified by resolution and extent of MS
92 processing.
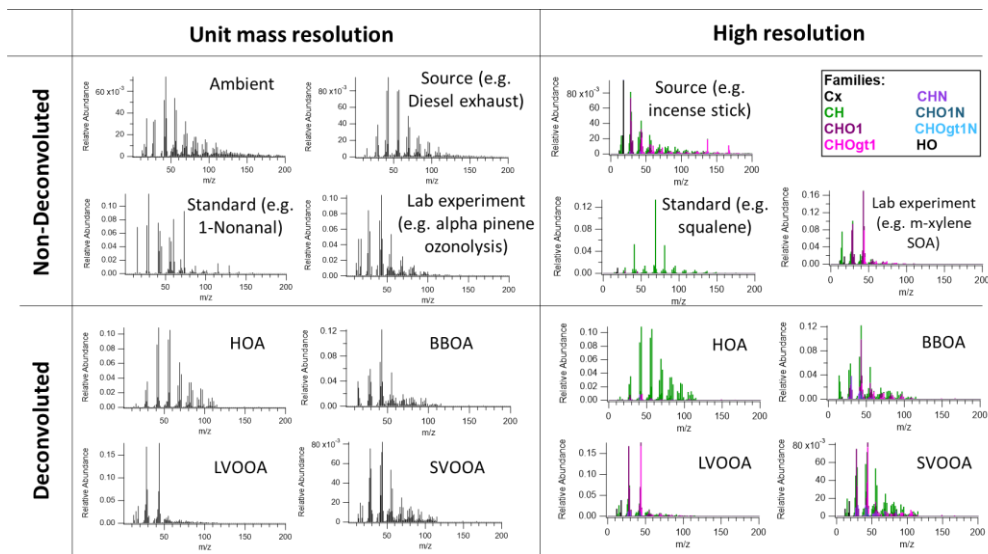
Figure 1. *Various examples of AMS OA mass spectral data divided by resolution and deconvolution. Each mass spectrum was plotted via the developed AMS MS comparison panel here and original data were from Alfarra et al., (2004); Canagaratna et al., (2004); Katrib et al., (2004); Bahreini et al., (2005); Li et al., (2012); Loza et al., (2012) for non-deconvoluted MS and Mohr et al., (2012) for deconvoluted MS.*

With existing datasets growing in complexity and number according to the advancement and accessibility of technology in the aerosol science field, it is increasingly important to develop customizable databases that store previous observations and act as a reference for future studies. Previous AMS and ACSM data have often been provided in text and graphical form, such as peer-reviewed journal publications. However, as the amount of data grows, finding the appropriate data in a usable format is increasingly challenging. Previous efforts to build a database for AMS and ACSM have been made by Ulbrich et al., (2009). They collected published AMS and ACSM spectral data and metadata (e.g., instrument operating conditions, sample, and experiment details), and posted it on an open-access website (https://cires1.colorado.edu/jimenez-group/AMSsd/). The digital data was uploaded as an Igor Pro software (Wavemetrics, Portland, OR) text file format, with an .itx file name extension. This allows users to load or export the data in the Igor Pro software commonly used for AMS and ACSM data analysis. This is a useful repository to advertise and distribute AMS and ACSM data. However, this repository is not programmed or formatted to systematically search for appropriate results and compare them with the researcher's own data. Beyond the need to program a search method, formatting needs to be standardized compared to the current method where each spectral data is individually uploaded on the webpage with some variability in format (e.g., variable mass-to-charge (*m/z*) ranges).

In this study, we introduce a searchable database tool for the AMS and ACSM mass spectral dataset. Our aim is to improve the efficiency and utility of the AMS and ACSM data analysis process, building on the existing database from Ulbrich et al., (2009). We converted the web-based database to a software-based database format using Igor-pro and developed the Igor Pro visualization interface. The interface is called 'AMS MS comparison panel' or simply 'panel' in the following sections. To demonstrate the practical application of this tool, we compared our AMS MS with reference MS in the database. This comparison demonstrates how our tool can be useful in practical applications. We believe that incorporating this comparison tool will enhance the ability of AMS and ACSM users to conveniently compare their data with previously reported studies.

2. Methods

The developed database is based on the existing open-access website by Ulbrich et al., (2009), providing published AMS and ACSM mass spectral datasets. The website mainly consists of 3 separate web pages such as unit mass resolution

123 (UMR, standard vaporizer), high resolution (HR, standard vaporizer), and capture vaporizer (CV, both UMR, and HR). Capture
124 vaporizer indicates that a more recently developed particle vaporizer was installed, which can lead to different spectra primarily
125 from increased thermal decomposition (Hu et al., 2018a). For each sample, the website provides metadata in a table format
126 including spectra identification, sources, research groups, AMS instruments used, electron ionization (EI) energy, and vaporizer
127 temperature. It also provides citation information and the original figure number in the publication, sometimes with additional
128 comments. The mass spectrum is uploaded in a digital form for analysis as an .itx file, a plain text file that can be directly
129 loaded into the data analysis software Igor-Pro (Wavemetrics, Portland, OR).

130 Here, to convert this web-based information and individual mass spectrum files to the software-based database in Igor-
131 Pro, the given information was fetched from HTML using the 'fetchURL' function in Igor-Pro to convert the contents of the
132 HTML to strings. Metadata was extracted from these HTML strings and saved in Igor Pro. Each mass spectrum was
133 automatically downloaded to the computer first and then saved in the Igor-Pro database. When saving the mass spectrum, it
134 was aligned and normalized in a uniform format with a consistent m/z range from 1 to 600 and a sum of the spectrum summing
135 to a value of 1. In the case of high resolution MS, they were converted to a UMR mass spectrum to make the HR mass spectrum
136 directly comparable to the UMR mass spectrum, and then also saved into the Igor-Pro database. HR ion family data was also
137 converted to UMR form and saved using the same method. For example, if the HR mass spectrum has three ions as CO_2^+ (m/z
138 43.9898), $C_2H_4O^+$ (m/z 44.0262), and $C_3H_8^+$ (m/z 44.0626), all these three ions are considered as m/z 44 on the database panel
139 in both UMR and HR. However, for HR ion families, these ions are respectively saved to corresponding HR ion families such
140 as CHOgt1, CHO1, and CH (a detailed description of HR families is presented in Table S1). After creating the software-based
141 database, the visualization interface (i.e., AMS MS comparison panel) was constructed in Igor Pro to analyze the correlation
142 between MS.

143

144 2.1 Mass spectrum correlation calculation

145 The main goal of this comparison panel is to provide a convenient function to analyze similarities between the mass
146 spectrum of interest and the reference MS in the database. In this comparison tool, we chose cosine similarity to estimate mass
147 spectrum similarity. Cosine similarity has been proved to show better performance in calculating correlations between MS
148 compared to other methods (Stein and Scott, 1994; Ulbrich et al., 2009). Therefore, it is commonly used to analyze the similarity
149 between MS in analyses of AMS spectra, referring to it as the dot product with normalized spectra input or uncentered
150 correlation coefficient (e.g. Marcolli et al., 2006; Lambe et al., 2015; Day et al., 2022). On the panel here, cosine similarity is
151 referred to as the 'Cosine score'. It measures the cosine of the angle between two vectors and is calculated by using the equation
152 below.

153
$$Cosine\ score\ =\ cos\ (\theta)\ =\ \frac{A \cdot B}{\|A\|\|B\|} \quad \text{(Eqn. 1)}$$

154 where each vector A and B are corresponding to the mass spectrum of interest and each reference mass spectrum in the database,
155 respectively. $\|A\|$ and $\|B\|$ denote the magnitudes of vectors A and B, and $A \cdot B$ indicates the dot product of A and B. The possible
156 range of cosine similarity (score) is from 0 to 1, and the higher the score value, the higher the similarity between the MS.

157 In addition, the panel supplies the option to reweight the mass spectrum using Equation 2 below. Regarding the
158 comparison of MS, instrument operation parameters can cause m/z-dependent differences in the amount or detection of ions,
159 and preprocessing spectral intensities by reweighting can have a beneficial effect on improving correlations between acquisition
160 methods (Stein and Scott, 1994). The score can be adjusted by varying their mass weighting and intensity scaling factors.
161 Increasing the relative significance of the lower-abundance high m/z values can enhance the match-weighting of these more
162 distinctive ions (i.e., molecular fragments). This is achieved by increasing the mass exponent (mass weighting) or decreasing
163 the peak intensity exponent (intensity scaling factors) that corresponds to the m and n in Equation 2, respectively.

164
$$Weighted\ intensity = [m/z]^m [Peak\ intensity]^n \quad \text{(Eqn. 2)}$$

165 The weighted exponents default to $m=0$ and $n=1$ on the panel. After reweighting, the mass spectrum is normalized by dividing
166 each value by the sum of the reweighted mass spectrum (thus summing to unity again). Finally, the panel calculates the score
167 using the scaled mass spectrum.

168 For HR mass spectral data, the score can be calculated with only the selected HR families on the panel. For example,
169 if one selects three HR families out of 17, then it combines these three HR family MS of interest into one mass spectrum and
170 sums to unity for normalization. It then calculates the score with a normalized mass spectrum utilizing the same method
171 described above. Detailed HR family information will be described in the next section. This score is referred to as 'Score with
172 HR family' on the HR data comparison tab of the panel.

173

174 **2.2 Igor AMS mass spectral comparison panel**

175 2.2.1 Data Comparison tab

176   Figure 2 shows a screenshot of the AMS MS comparison panel. The panel is divided into four tabs (dashed line in
177 orange of Figure 2): i) UMR Data comparison, ii) UMR Database, iii) HR Data comparison, and iv) HR Database. Both data
178 comparison tabs for UMR and HR data consist of three regions. Figure panel section 2a (highlighted in blue) is where a new
179 or existing mass spectrum is selected for comparison against database MS. Section 2b (highlighted in red) is where the user
180 will set search parameters and view results, and section 2c (highlighted in black) is where metadata of selected database
181 components can be viewed. Screenshots of other tabs are shown in the supplementary material (Figs. S1-3).

182
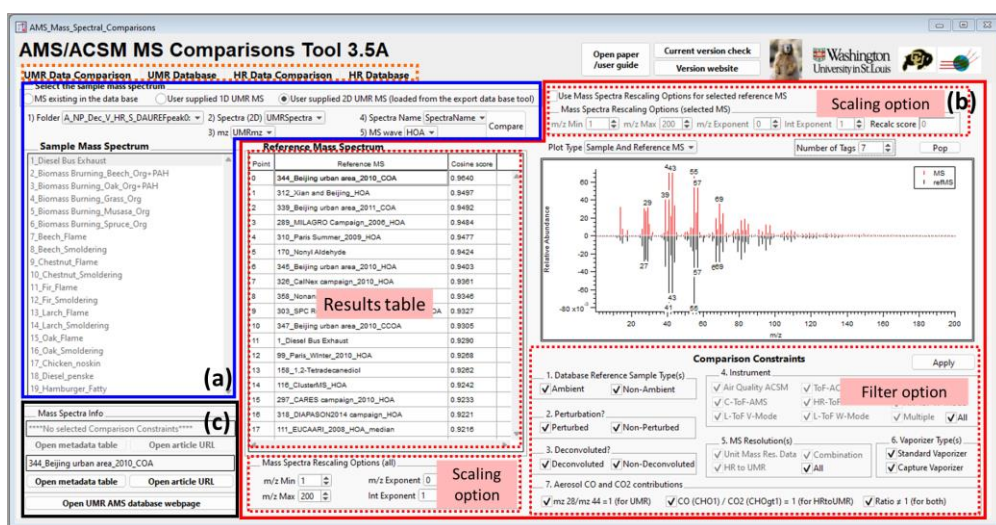
183

184 *Figure 2. A screenshot of the UMR Data comparison tab in the 'AMS MS Comparison Panel'. In box (a), the user selects their*
185 *sample mass spectrum of interest, in box (b) the user views a comparison result of the sample with the database reference mass*
186 *spectrum and sets the scaling option and filter option, and the box (c) provides the citation information.*

187   In panel section 2a, users are able to select MS to be compared. There are two options for users to choose a mass
188 spectrum of interest. One is to choose their own mass spectrum ('User supplied 1D/2D UMR MS'), and the other is to select
189 an existing mass spectrum in the database ('MS existing in the data base'). In the case of selecting their own mass spectrum,
190 the mass spectrum has to be in UMR with a standard m/z range. The current panel and database use a mass range of m/z 1-600.
191 Detailed information on how to upload the user's own data to the database panel is described in the user guide section (Chapter
192 2 for UMR and Chapter 3 for HR) of the supplementary information.

193   Panel section 2b contains the results table, mass spectrum plots window, scaling mass spectrum options, and
194 comparison filter options. The results table shows the list of reference spectra sorted by the calculated score (cosine similarity)
195 in descending order. Users are able to see the reference spectrum of interest on the mass spectrum plots window by clicking on
196 the results table. For the UMR data comparison tab, the mass spectrum plot window provides five types of mass spectrum plots
197 (selectable with the "Plot Type" drop-down above the plot shown in Fig. 2: sample mass spectrum of interest, reference mass
198 spectrum selected, mirror-image sample and reference MS, subtraction of sample and reference MS, and the scatter plot
199 between the sample and reference with the markers corresponding to the specific m/z value with regression information (Fig.
200 3). For the HR data comparison tab, the panel plots a stacked mass spectrum with HR ion families such as Cx, CH, CHO1,
201 CHOgt1, etc (Fig. S2b). These HR ion families are the same names generated by PIKA v1.23B which is an AMS data analysis
202 tool for HR (DeCarlo et al., 2006; Sueper, 2021, https://cires1.colorado.edu/jimenez-group/ToFAMSResources/ToFSoftware/).
203 The chemical formula for each HR ion family is described in Table S1. Users can select the HR ion family to be viewed on the

204 window and can calculate a 'score with HR family' with these selected HR families to compare the mass spectrum specifically.
205 These various types of plots will help users visually observe the similarities and differences between the MS. The scaling mass
206 spectrum option can reset the mass range and reweight the mass spectrum. Users are able to choose whether to apply the scaling
207 options to all reference MS in the database (below the results table in panel section 2b) or to only one selected reference mass
208 spectrum on the list (top right of the panel in panel section 2b) in UMR data comparison tab. For HR data, it only provides the
209 scaling option for all reference MS. Furthermore, the panel supplies comparison constraints to filter the reference MS in the
210 database depending on the metadata. Comparison constraint categories include sample type, perturbation, deconvolution,
211 instrument, MS resolution, and CO and CO_2 contribution sections. Detailed descriptions of these constraints are provided in
212 the supplementary material (Section S1).
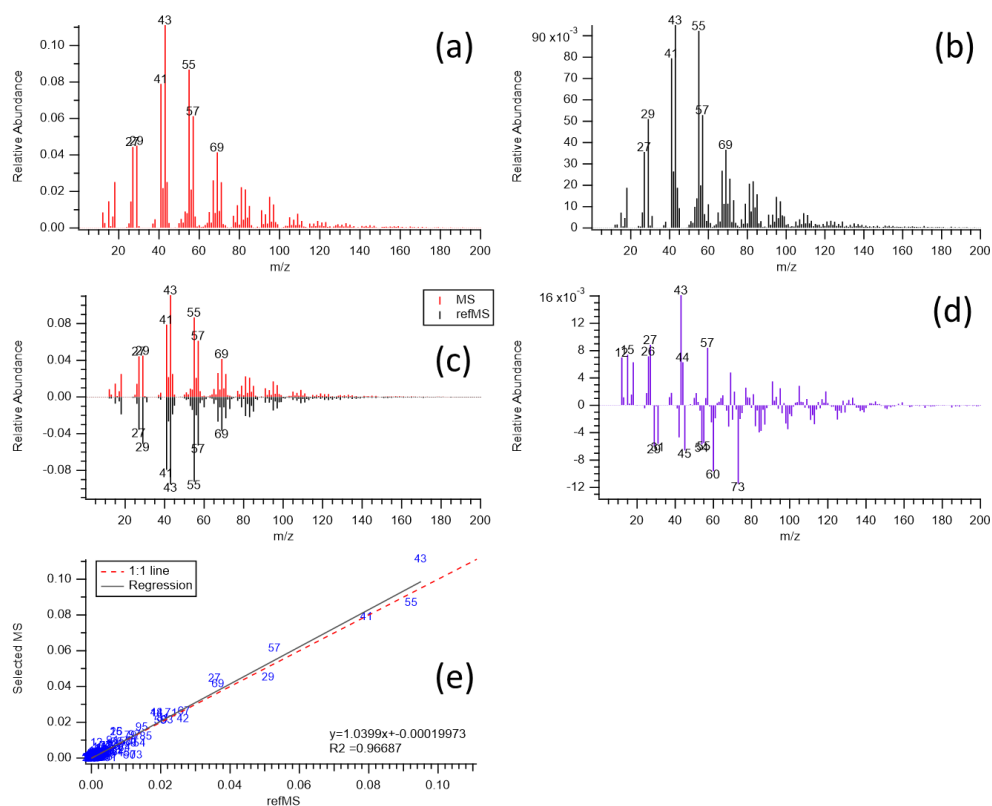
213

214 *Figure 3. Five types of plots provided by the panel to inform mass spectral comparisons: (a) sample mass spectrum of interest,*
215 *(b) reference mass spectrum selected, (c) mirrored-image sample and reference MS, (d) subtraction (difference) of sample and*
216 *reference MS, and (e) scatter plot between the sample and reference mass spectrum with the markers corresponding to the*
217 *specific m/z values with regression information. Original data were from Ulbrich et al., (2009) and Mohr et al., (2009). In this*
218 *example (as observed in panel d) the sample MS (HOA) contains additional m/z 43 and 57 (both of which have primary or*
219 *secondary contributions and would need to further explore the HR results to distinguish), and the reference MS (laboratory,*
220 *chicken cooking without skin) contains additional m/z 60 and 73 (common biomass markers or carboxylic acids).*

221

222   Finally, in panel section 2c, users can find detailed information on the sample mass spectrum of interest and selected
223 reference MS in the results table. The "Open metadata table" button in panel section 2c enables a new window to pop up for
224 users to obtain information. The new window shows sample type, perturbed type, analysis, instrument type, resolution,

225 vaporizer type, EI energy value, vaporizer temperature, experimenter's name, group, citations, citation URLs, figure numbers
226 in the citation, and related comments (Fig. S4). In addition, users can directly open the relevant published paper in a web
227 browser via the panel ("Open article URL" button in panel section 2c) if the URL address of the paper is saved in the database.

229 2.2.2 Database tab

230 Both database tabs of UMR and HR (Figs. S1, S3) display reference MS in the database. Users can simply observe
231 the reference mass spectrum in the database with metadata without correlation calculation. Users can scan the MS stored in the
232 database through this tab and easily obtain the corresponding reference metadata.

234 **3. Application of the AMS MS database and comparison panel**

235 Here, we used PMF factor mass spectral data from the DAURE campaign (Determination of the sources of
236 atmospheric Aerosols in Urban and Rural Environments) to display the utility of the developed database and comparison panel.
237 Data for this study were acquired in high resolution during the intensive DAURE field campaign in Montseny, Spain, during
238 February-March 2009. An 8-factor solution (FPEAK=0) was chosen since this was the lowest number of factors at which the
239 HOA and BBOA factors showed a clear separation from each other and OOA. Six factors were recombined to make up the
240 OOA factor. The BBOA and HOA factors used here are those from the 8-factor solution. More details about an overview of
241 the DAURE campaign and a summary of the results can be found in Minguillón et al., (2011), Pandolfi et al., (2014), and
242 Zhang et al., (2022). For comparison, the acquired PMF factor mass spectral data in HR was converted to a UMR mass
243 spectrum. Figure 4 shows the converted PMF factor MS of HOA, BBOA, and combined OOA in UMR and stacked HR ion
244 families, respectively. In this section, we will introduce examples of ways to utilize the new comparison panel by applying
245 functions via the UMR data comparison tab and present a potential for the HR data comparison tab based on HR families and
246 'score with HR family' to obtain more information to interpret the data depending on our factor MS.
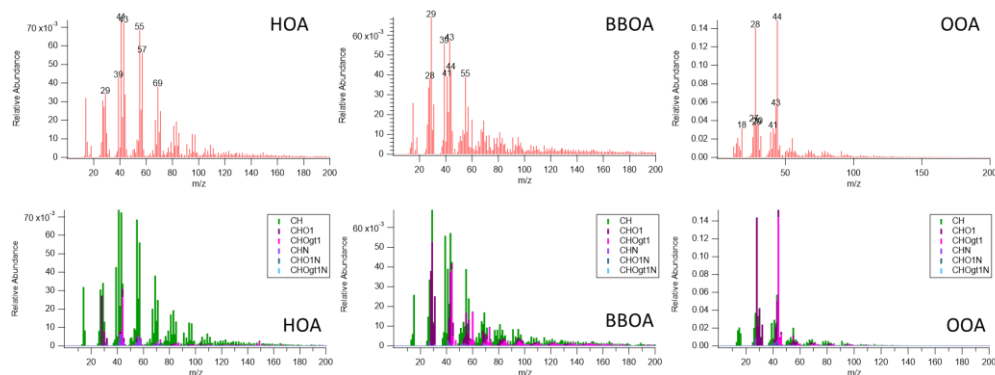
249 *Figure 4. PMF factor MS from Montseny, Spain during the DAURE campaign (Minguillón et al., 2011) in UMR and stacked*
250 *HR ion families. The acquired PMF factor MS in high resolution were converted to a UMR mass spectrum and plotted by the*
251 *AMS MS comparison panel here.*

253 As introduced above, the developed database panel provides different ways to compare the MS with filtering or scaling
254 options. Among these options, the 'sample type' category in the filtering option (Fig. 2. section b) enables researchers to select
255 'ambient' or 'non-ambient' samples in the database. The 'Ambient' option indicates direct measurement of ambient air and the
256 'non-ambient' option includes analysis of chamber studies, source emission studies, standards, etc. The scaling option is used
257 to scale the mass spectrum using the mass range, mass exponent, and intensity exponent based on Eqn. 2. The default setting
258 of the scaling option on the panel is $m=0$ and $n=1$ on Eqn. 2. The comparison process and results for each method will be
259 described in this section with the DAURE campaign PMF factor MS as an example.

Selecting the 'ambient' option is useful when the user wants to compare their mass spectrum only with previous ambient measurements. For example, after the final PMF factors are identified, we may want to confirm if the identified PMF factors have a similar MS compared with previous studies. In this case, users can apply the 'ambient' sample filter to compare. Table 1 shows the comparison results with the cosine similarity when we executed a UMR comparison of the HOA factor identified from the DAURE campaign (Montseny, Spain) with the database as an example. In the results table, most of the samples in the database with a score greater than 0.9 were shown as 'HOA'. An interesting observation that appears is that some cooking organic aerosol (COA) factors also showed a high correlation with our HOA factor. The COA factor is often identified by its characteristic mass fragment of m/z 55, and it also has the same hydrocarbon ion series (m/z 29, 43, 57, 71, for $C_nH_{2n+1}^+$ and m/z 41, 55, 69, for $C_nH_{2n-1}^+$) as the HOA (Mohr et al., 2009). The HOA factor we compared has a large m/z 55 in the spectrum and that may be the main cause for some COA factors to score a high match. Therefore, we would conclude that our HOA factor might be mixed with cooking sources. However, in this case, if the user has HR family information of the mass spectrum, as we do here, one could have more information to interpret the result.

COA factor MS usually have a relatively high portion of CHO1 family in m/z 55 compared to HOA, which would be from the $C_3H_3O^+$ ion (Mohr et al., 2009, 2012). Figure 5 shows the comparisons of m/z 55 in stacked HR families with the top 3 reference samples in Table 1. The m/z 55 in our HOA and Xian and Beijing HOA factor MS mainly consists of CH family, specifically $C_4H_7^+$, and this contribution is clearly distinguished from the COA reference MS such as Beijing urban area 2010 and 2011 having larger m/z 55 contributions from CHO1 family, specifically $C_3H_3O^+$. These trends are also shown in Mohr et al., (2012) where AMS data acquired during the field campaign DAURE in Barcelona, Spain were analyzed and HOA and COA were both separated as a result. The HOA factor mass spectrum in Mohr et al., (2012) also had the m/z 55 only slightly smaller than m/z 57. However, the m/z 55 in their HOA factor mass spectrum is also predominantly contributed from the CH family as we observed here. Likewise, in their COA factor mass spectrum, m/z 55 is much larger than m/z 57 and nearly half of m/z 55 was from the CHO1 family. Therefore, we may conclude that our HOA factor is most similar to previous 'HOA' MS even if it has a high abundance of m/z 55. However, it also suggested that additional PMF analysis with more factors could find some contribution of COA mixed in our HOA that could perhaps be separated. This comparison shows the strength of incorporating the HR families available from HR-AMS datasets as well as simple UMR ambient comparison via the panel.

Table 1. Top matches from "Ambient" sample UMR comparison results with HOA factor from the DAURE campaign (m/z 1-200)

# in DB	Sample	Score	Reference
311	Beijing urban area_2010_COA	0.9640	(Hu et al., 2016)
279	Xian and Beijing_HOA	0.9497	(Elser et al., 2016)
306	Beijing urban area_2011_COA	0.9492	(Hu et al., 2016)
253	MILAGRO Campaign_2006_HOA	0.9483	(Alfarra et al., 2004)
277	Paris Summer_2009_HOA	0.9477	(Crippa et al., 2013)
312	Beijing urban area_2010_HOA	0.9403	(Hu et al., 2016)
293	CalNex campaign_2010_HOA	0.9361	(Hayes et al., 2013)
270	SPC Research Station Po Valley_2008_HOA	0.9327	(Saarikoski et al., 2012)
314	Beijing urban area_2010_CCOA	0.9305	(Hu et al., 2016)
101	Paris_Winter_2010_HOA	0.9269	(Crippa et al., 2013)
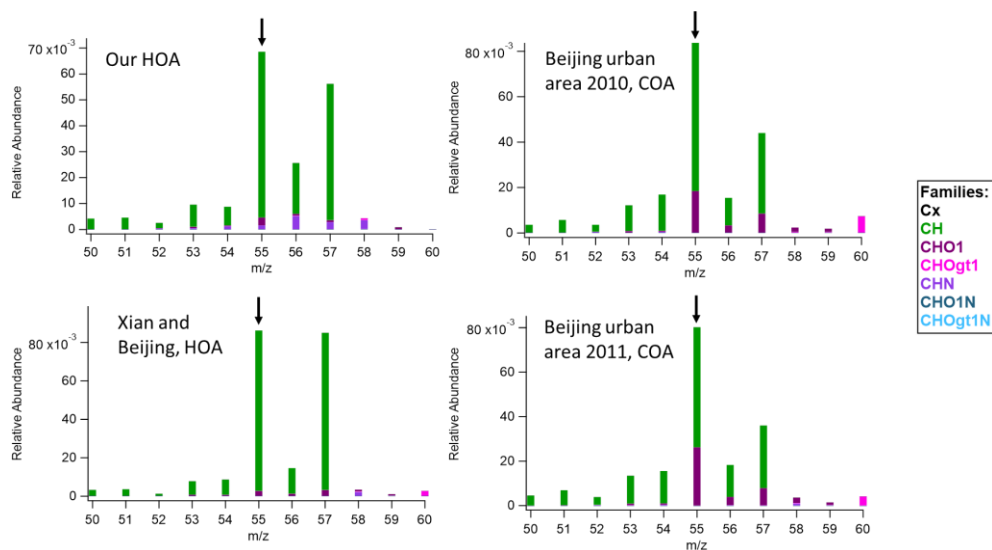
Figure 5. Segments of the MS (m/z 50-60) for our HOA and top 3 reference samples that correlated highly with our HOA in the "Ambient" comparison for m/z 55 HR ion families

'Non-ambient' option is convenient to compare the mass spectrum of interest with laboratory samples in the database. For example, this option is helpful when comparing a mass spectrum derived from a specific source such as BBOA. When applying the non-ambient filtering option, several non-ambient reference MS were highly correlated with our BBOA MS (Table 2). The characteristic mass fragment of BBOA is m/z 60 attributed to $C_2H_4O_2^+$ (from anhydrous sugars such as levoglucosan) and this specific ion was observed in most of the MS in the list of high score matches. On the HR data comparison tab, we are able to confirm if the m/z 60 is from the oxygenated HR family (CHOgt1). In Table 2, only the mosquito coil sample included HR ion family data and we confirmed the m/z 60 was mostly from CHOgt1 ion family which is pink (Fig. 6). Since the main component of mosquito coil is biomass such as sawdust, coconut shell flour, pyrethrum, potato starch, etc, it seems to show a high correlation with our BBOA and similar HR ion family contribution in m/z 60.

Table 2. Top matches from "Non-ambient" sample UMR comparison results with the BBOA factor from the DAURE campaign (m/z 1-200)

# in DB	Sample	Score	Reference
30	Ponderosa Pine Duff	0.9404	(FLAME, 2007)
41	Puerto Rican Mixed Wood	0.9337	
40	Southern Pine Needles	0.9335	
325	Mosquito Coil	0.9303	(Li et al., 2012)
38	Puerto Rican Fern	0.9296	(FLAME, 2007)
31	Alaska Core Tundra Duff	0.9275	
36	Ceanothus Leaves and Berries	0.9193	
27	Ponderosa Pine Needles and Sticks	0.9184	
39	Wax Myrtle	0.9038	
35	Lignin Powder	0.8951	
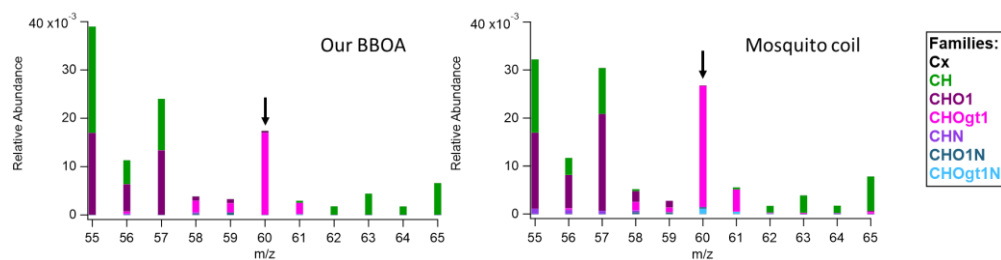
Figure 6. Enlarged MS of our BBOA and mosquito coil sample for m/z 60 HR ion family

An interesting observation from BBOA example is that when carrying out the ambient sample comparison with the BBOA factor, other identifications such as HOA, SVOOA, LOOOA, COA, etc were observed as well as BBOA (Table 3) even though our BBOA mass spectrum was highly correlated with biomass burning laboratory references. Since ion separation of AMS mass spectrum via PMF is largely impacted by the mix of sources present at a given time, users don't always obtain a 'perfectly separated' mass spectrum identifying the mass spectrum as HOA, BBOA, COA, etc, but a possibly mixed mass spectrum. It indicates that even if the UMR score on the panel is lower, it could be possible that there is a good match with a single HR family or some families, and vice versa. For this case, 'Score with HR family' can be a useful function to gain more information on similarities. When users select the HR families of interest next to the HR plot window and click the calculate button below HR family selection, it combines only the selected HR families into one MS, calculates a cosine similarity in the same way, and displays the results named 'score with HR family' on the results table. Table 3 shows top 10 matches from ambient sample comparison results sorted by the UMR score and top 10 matches from 'score with HR family'. For BBOA, the separation of the oxygenated ions provides a lot of information and is a key signature of BBOA spectra. On Table 3, we were able to observe more BBOA factor mass spectrum on the list when sorting the results by the score with CHOgt1 family including *m/z* 60. Most of the new matches showed BBOA, CCOA (coal combustion OA), HOA, and COA, not OOA like when sorting the list by UMR score. UMR match scores for these reference MS are included alongside the HR Family match score for comparison. We also carried out a score comparison utilizing additional HR families and family combinations (CH, CHO1, and combined), but it did not provide additional insight beyond what was observed with CHOgt1 alone (Table S2).

Table 3. Top matches from HR "Ambient" sample comparison results with the BBOA factor from the DAURE campaign (m/z 1-200) depending on UMR score and score with HR family (CHOgt1)

# in DB	Sample	UMR score		Reference
Top 10 matches sorted by UMR score				
293	Changdao island_2011_biomass burning	0.9632		(Hu et al., 2013)
310	SOAS campaign_2013_SOA	0.9445		(Hu et al., 2015)
300	Beijing urban area_2011_HOA	0.9367		(Hu et al., 2016)
245	SOAR-1_Campaign_2005_SVOOA	0.9346		(Docherty et al., 2011)
313	SOAS campaign_2013_LOOOA_II	0.9287		(Hu et al., 2015)
296	Changdao island_2011_CCOA	0.9239		(Hu et al., 2013)
315	KORUS-AQ study_2016_LOOOA	0.9164		(Hu et al., 2018b)
269	Paris Summer_2009_SVOOA	0.9149		(Crippa et al., 2013)
301	Beijing urban area_2011_COA	0.9097		(Hu et al., 2016)
265	SPC Research Station Po Valley_2008_HOA	0.9050		(Saarikoski et al., 2012)
Top 10 matches sorted by the score with HR family (CHOgt1)				
# in DB	Sample	UMR score	Score with CHOgt1	Reference
254	DAURE campaign_2009_BBOA	0.8348	0.9527	(Mohr et al., 2012)

296	Changdao island_2011_CCOA	0.9239	0.9265	(Hu et al., 2013)
259	CARES campaign_2010_HOA	0.8384	0.9216	(Setyan et al., 2012)
268	Paris Summer_2009_COA	0.8231	0.9208	(Crippa et al., 2013)
275	Xian and Beijing_COA	0.8311	0.9195	(Elser et al., 2016)
283	POPE2014 campaign_COA	0.7947	0.9079	(Struckmeier et al., 2016)
266	SPC Research Station Po Valley_2008_BBOA	0.8913	0.9061	(Saarikoski et al., 2012)
304	Beijing urban area_2010_LVOOA	0.8474	0.9052	(Hu et al., 2016)
293	Changdao island_2011_biomass burning	0.9632	0.9045	(Hu et al., 2013)
307	Beijing urban area_2010_HOA	0.8496	0.8995	(Hu et al., 2016)

Lastly, users can use the "scaling mass spectrum" feature, which is especially helpful for up-weighting signal intensity of larger and more unique ions by increasing the mass exponent value or decreasing the intensity exponent value. When we compared the OOA factor MS with ambient samples, we observed that our OOA factor MS was highly correlated with LVOOA (or MOOOA) MS from previous studies (Table S3) showing a score of more than 0.97. We also explored cosine scores of the OOA factor with non-ambient spectra within the database. However, when we compared the OOA factor MS with non-ambient samples, top scores in the list were shown as less than 0.9 (Table 4). For OOA, the abundances of fragment ions m/z 28 (CO^+) and 44 (CO_2^+) are extremely dominant compared to other ions in the mass spectrum (typically, the m/z 28 signal is constrained to be equal to the m/z 44 signal). These prominent abundances of a few spectral peaks may affect score calculation. In the case of 'ambient' comparison with deconvoluted MS dominated by m/z 28 and 44, signals from other ions may not highly influence the results as shown in Table S3. On the other hand, in the case of 'non-ambient' comparison with non-deconvoluted MS dominated by m/z 28 and m/z 44 signals of laboratory samples, signals from other ions are more unique to the specific laboratory conditions and may reflect the lower scores as shown in Table 4. In this case, we have two options to reduce these impacts on score results: i) increase the m/z exponent value, ii) decrease the intensity exponent value, or iii) both i and ii in Eqn 2.

Table 4. Top matches from UMR "Non-ambient" sample comparison results with the OOA factor from the DAURE campaign (default setting, m/z 1-200)

# in DB	Sample	Score	Reference
141	Oxalic acid	0.8493	(Takegawa et al., 2007)
334	Chamber m-Xylene aged SOA	0.8458	(Loza et al., 2012)
321	Incense Coil	0.8385	(Li et al., 2012)
145	Adipic acid	0.8196	(Takegawa et al., 2007)
149	Glyoxylic acid	0.8132	(Takegawa et al., 2007)
331	Citric Acid (C8H8O7)	0.7661	(Hu et al., 2018b)
143	Succinic acid	0.7649	(Takegawa et al., 2007)
234	Diesel_Exhaust_2	0.7629	(Sage et al., 2008)
322	Mosquito Coil	0.7580	(Li et al., 2012)
333	Chamber m-Xylene peak growth SOA	0.7529	(Loza et al., 2012)

Figure 7 shows the reweighted OOA mass spectrum generated by two exponent options. When we increased the m/z exponent from 0 to 1 (Figure 7b), we observed that the relative abundance of lower mass fragments decreased and that of larger mass fragments increased in a similar scale of relative abundance as the original MS (Figure 7a). When we decreased the peak intensity exponent from 1 to 0.5 (Figure 7c), the maximum value of relative abundance was decreased. Signal intensities other than the dominant fragments (m/z 28 and 44) were more balanced than in Figure 7a. Figure 7d is the case where we applied both mass and peak intensity exponent options. It shows the reweighted spectra with relatively smaller contributions from lower masses and higher contributions from larger masses. Table 5 shows the list of reference MS with a high correlation with our reweighted OOA factor MS with various pairs of m/z and peak intensity exponent. The scores less than 0.9 were not shown in the table and the reference samples were sorted by the maximum score among the values from each scenario. It shows that for our OOA factor MS, decreasing the intensity exponent option resulted in more scores greater than 0.9 compared to increasing the m/z exponent. Also, we observed that the reweighted OOA factor mass spectrum is mostly correlated with coils, terpene ozonolysis, aged SOA, etc. Correlations to the coils may be because both incense coil and mosquito coil have fragrances that contain aromatic compounds that can produce oxygenated aromatics during combustion.

359
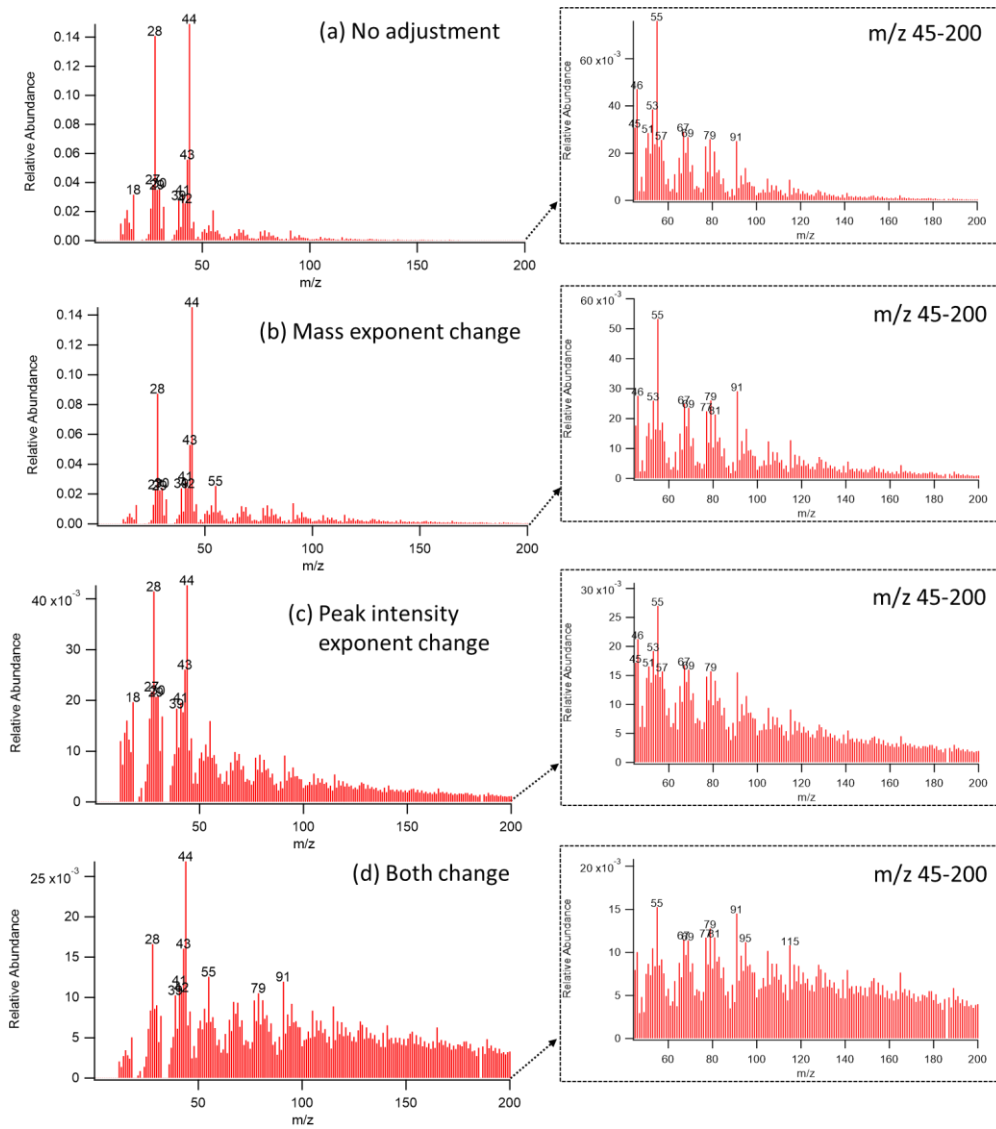
Figure 7. The reweighted mass spectrum of DAURE OOA factor ((a): No adjustment, (b): increase m/z exponent from 0 to 1, (c): decrease intensity exponent from 1 to 0.5, and (d): apply (b) and (c) simultaneously). Enlarged mass spectrum with a restricted mass range (m/z 45-200) shown in the dashed line box.

Table 5. Top matches from "Non-ambient" UMR sample comparison results with the OOA factor from the DAURE campaign depending on decreasing peak intensity exponent and increasing mass exponent. The maximum score is shown in bold.

m/z exponent		0	1	1	
Peak intensity exponent		0.5	1	0.5	
# in DB	Sample	Score			Reference
321	Incense Coil	**0.9413**	-	0.9316	(Li et al., 2012)
334	Chamber m-Xylene aged SOA	**0.9306**	-		(Loza et al., 2012)
212	Myrcene_O3	-	-	**0.9252**	(Bahreini et al., 2005)
322	Mosquito Coil	0.9149	-	**0.9199**	(Li et al., 2012)
222	Myrcene_O3	-	-	**0.9176**	(Bahreini et al., 2005)
32	Utah Sage, Rabbitbrush	-	-	**0.9174**	(FLAME, 2007)
213	Terpinolene_O3	-	-	**0.9157**	(Bahreini et al., 2005)
31	Utah Juniper Foliage and Sticks	-	-	**0.9151**	(FLAME, 2007)
205	beta-caryophyllene_O3	-	-	**0.9151**	(Bahreini et al., 2005)
130	Fulvic Acid	-	-	**0.9142**	(Alfarra, 2004)

Setting a restricted mass range is another way to modify the score. Table 6 shows the scores of our reweighted OOA MS when setting a new mass range from m/z 45 to 200 and changing the mass and the peak intensity exponent, respectively. Increasing the mass range parameter was generally helpful to explore comparisons beyond the dominant m/z 28 and m/z 44 signals. Decreasing the peak intensity exponent showed higher scores in the list compared to the case of increasing the mass exponent. However, for our OOA, the mass exponent change was more useful to emphasize specific larger ions such as m/z 55, 91, and 115 shown in the enlarged mass spectrum in a dashed box of Figure 7b. We observed that the higher m/z range in the reweighted OOA mass spectrum is highly correlated with terpene ozonolysis and biomass burning (Table 6).

Table 6. Top matches from "Non-ambient" sample UMR comparison results with the reweighted OOA factor from the DAURE campaign depending on the pairs of mass and intensity exponent value with restricted mass range (m/z 45-200)

m/z exponent		0	0	1	1	
Peak intensity exponent		1	0.5	1	0.5	
# in DB	Sample	Score				Reference
217	Bcaryophyllene_O3	0.9097	0.9587	0.9292	**0.9723**	(Bahreini et al., 2005)
32	Utah Sage, Rabbitbrush	0.9052	0.9563	0.9277	**0.9696**	(FLAME, 2007)
205	beta-caryophyllene_O3		0.9586	0.9264	**0.9693**	(Bahreini et al., 2005)
212	Myrcene_O3		0.9596	0.9185	**0.9693**	(Bahreini et al., 2005)
31	Utah Juniper Foliage and Sticks			0.9218	**0.9668**	(FLAME, 2007)
222	Myrcene_O3		0.9568		**0.9667**	(Bahreini et al., 2005)
218	a-Humulene_O3	0.9165	0.9578	0.9285	**0.9651**	(Bahreini et al., 2005)
26	Southern CA Chamise				**0.9579**	(FLAME, 2007)
203	a-humulene_O3		0.9513	0.9156	**0.9538**	(Bahreini et al., 2005)
206	beta-pinene_O3	0.9139	**0.9538**	0.9258		(Bahreini et al., 2005)

In addition to the comparison of the combined OOA mass spectrum, we used these scaling options to check if each of the original 6 OOA-related factors had potential characteristics to be identified before they were combined. As a result of the application of a variety of paired scalings of mass range, mass exponent value, and intensity exponent value, we observed potential characteristics between factors when using the mass range is m/z 45-200 and default exponent value (m=0, n=1) (Table S4). In this case, factor 1 and factor 4 were highly correlated with the oxidation of m-xylene (an anthropogenic VOC common in fossil fuels) and other potential ozonolysis products, and factor 5 and factor 6 were mostly correlated with terpene ozonolysis. Factor 2 and factor 3 showed relatively lower scores but nitrogen-related MS was shown in the results table in both factors. These results suggest that we could combine factors 1 and 4, factors 2 and 3, and factors 5 and 6 as potential OOA subcategories. When we calculated cosine similarities between these pairs of factors, it showed a high correlation with the score of 0.9576, 0.9469, and 0.9838, respectively, which supports their similarities in composition. Factors 5 and 6, in particular, had characteristic fragment ion m/z 91 which can be indicative of monoterpene oxidation matching the results we obtained. Therefore, based on a new combination of factors, we may conclude that our OOA may be mainly derived from m-xylene

391 (anthropogenic VOC) oxidation, terpene ozonolysis, and nitrogen-related reactions. For HR data comparison, unfortunately,
392 all non-ambient samples in this match list were originally submitted only in UMR, so HR family comparison was not available
393 in this case. Importantly, future MS submissions from the user community should include HR MS when available.

394

4. Discussions

396 The existing AMS and ACSM mass spectral database in web-based form has been converted into a searchable,
397 filterable software library coupled with a comparison panel in Igor Pro, the main analysis program currently used for AMS and
398 ACSM data. The comparison panel provides the functionality to compare the mass spectrum of interest with MS in the database
399 statistically and visually by cosine similarity and several types of mass spectral plots as UMR or stacked HR ion families.
400 Furthermore, the option to exponentially reweight the mass spectrum and filter the samples depending on their measurement
401 information (e.g. lab vs field data) can help users understand and analyze their data relative to a growing list of past
402 observations. We believe this new database can be used to improve the efficiency of data interpretation and provide new insights
403 for AMS and ACSM studies. However, we highlight considerations that users should keep in mind when using this tool for
404 more accurate AMS and ACSM data interpretation. Initially, when users set a new mass range, users should take into account
405 the maximum m/z value of their target mass spectrum for comparison. As the maximum m/z values (having none-zero value)
406 of reference mass spectra in the database may vary, adjusting the mass range can impact the cosine score. In cases where there
407 are significant signals and distinctive peaks at the higher m/z range for the target spectrum, including the higher range may
408 help identify spectra in the database that may be similar if they also contain the higher m/z range. In addition, while MS are
409 one of the AMS and ACSM data to be used for data interpretation, users should continue to consider all supporting chemical
410 and meteorological measurements together with the AMS and ACSM MS in determining factor identities. For especially AMS
411 users, it's important to consider the instrumental conditions of reference mass spectra in the database, such as the instrument
412 analysis mode (e.g. W or V mode) and particle size range, as these factors can impact the mass spectrum during AMS data
413 processing. For instrument analysis mode, in this paper, we had a limited number of V-mode spectra which was the mode of
414 our target spectra, so we conducted comparisons using the entire database to demonstrate the tool's functionality. However,
415 since W-mode analysis may result in being able to more confidently fit ions due to its higher resolution than V-mode, the
416 correlation may be different when comparing to W-mode vs V-mode. To address this, our tool offers an instrument filtering
417 option, which we recommend to use for more precise AMS data interpretation. Particle size range (due to different aerodynamic
418 lens use), although not provided by this tool, can also influence the mass spectrum. To access this information, users can utilize
419 the metadata and reference paper available online via the panel. We encourage users to carefully review the reference paper for
420 particle size details and, if needed, additional information such as a fragmentation table for their data interpretation.

421 Lastly, the AMS and ACSM users' network should further populate this digital mass spectral database in order to fully
422 realize the potential strength of such a tool. Users can download the latest version of the database as a .h5 file and the procedure
423 file for this tool through the GitHub link on the existing AMS database webpage (https://cires1.colorado.edu/jimenez-
424 group/AMSsd/). Users can confirm the version of the database and procedure file they are using on the panel and update them
425 by downloading files at the link. Users can also follow the listed procedures for submitting new MS to the database and refer
426 to the user manual (see user guide section in supplementary material) to use this tool. As a variety of databases and tools (e.g.,
427 SoFi, SPECIEUROPE, and ICARUS) have been developed to enhance data analysis efficiency in the atmospheric field
428 (Canonaco et al., 2013; Pernigotti et al., 2016; Nguyen et al., 2023), we anticipate providing a valuable database and tool for
429 users as well. Our intention is that this database continues to grow and develop with the various types of AMS and ACSM
430 systems in operation and can serve as a useful tool to help AMS users frame their observations against a wealth of previous
431 observations obtained globally.

432

Code availability

434 The code of AMS mass spectral database in this study was developed in the Igor Pro environment. The codes are available at
435 https://github.com/ActlabW/AMS_MS_DB.

436

Data availability

438 AMS mass spectra data used in this study is available at https://cires1.colorado.edu/jimenez-group/AMSsd/.

439

Author contribution

SJ developed the software code and prepared the manuscript with constructive feedback from DTS and DAD. MJW conceptualized the project and framed the initial code. DTS and DAD contributed to inspecting the tool and the database. DTS, DAD, AVH, and JLJ supplied AMS mass spectral data. BJW supervised the project. All authors participated in reviewing and editing the manuscript.

Competing interests

The contact author has declared that none of the authors has any competing interests.

Acknowledgments

BJW acknowledges NSF CBET (award number 1554061) for supporting this study. DTS, AVH, DAD, JLJ acknowledge support from NASA 80NSSC21K1451 and NSF AGS AGS-2131914 and 2206655.

References

Adam, T. W., Chirico, R., Clairotte, M., Elsasser, M., Manfredi, U., Martini, G., Sklorz, M., Streibel, T., Heringa, M. F., DeCarlo, P. F., Baltensperger, U., De Santi, G., Krasenbrink, A., Zimmermann, R., Prevot, A. S. H., and Astorga, C.: Application of Modern Online Instrumentation for Chemical Analysis of Gas and Particulate Phases of Exhaust at the European Commission Heavy-Duty Vehicle Emission Laboratory, Anal. Chem., 83, 67–76, https://doi.org/10.1021/ac101859u, 2011.

Aiken, A. C., DeCarlo, P. F., Kroll, J. H., Worsnop, D. R., Huffman, J. A., Docherty, K. S., Ulbrich, I. M., Mohr, C., Kimmel, J. R., Sueper, D., Sun, Y., Zhang, Q., Trimborn, A., Northway, M., Ziemann, P. J., Canagaratna, M. R., Onasch, T. B., Alfarra, M. R., Prevot, A. S. H., Dommen, J., Duplissy, J., Metzger, A., Baltensperger, U., and Jimenez, J. L.: O/C and OM/OC Ratios of Primary, Secondary, and Ambient Organic Aerosols with High-Resolution Time-of-Flight Aerosol Mass Spectrometry, Environ. Sci. Technol., 42, 4478–4485, https://doi.org/10.1021/es703009q, 2008.

Aiken, A. C., Salcedo, D., Cubison, M. J., Huffman, J. A., DeCarlo, P. F., Ulbrich, I. M., Docherty, K. S., Sueper, D., Kimmel, J. R., Worsnop, D. R., Trimborn, A., Northway, M., Stone, E. A., Schauer, J. J., Volkamer, R. M., Fortner, E., de Foy, B., Wang, J., Laskin, A., Shutthanandan, V., Zheng, J., Zhang, R., Gaffney, J., Marley, N. A., Paredes-Miranda, G., Arnott, W. P., Molina, L. T., Sosa, G., and Jimenez, J. L.: Mexico City aerosol analysis during MILAGRO using high resolution aerosol mass spectrometry at the urban supersite (T0) – Part 1: Fine particle composition and organic source apportionment, Atmospheric Chemistry and Physics, 9, 6633–6653, https://doi.org/10.5194/acp-9-6633-2009, 2009.

Alfarra, M. R.: Insights into atmospheric organic aerosols using an aerosol mass spectrometer, PhD Thesis, University of Manchester, 2004.

Alfarra, M. R., Coe, H., Allan, J. D., Bower, K. N., Boudries, H., Canagaratna, M. R., Jimenez, J. L., Jayne, J. T., Garforth, A. A., Li, S.-M., and Worsnop, D. R.: Characterization of urban and rural organic particulate in the Lower Fraser Valley using two Aerodyne Aerosol Mass Spectrometers, Atmospheric Environment, 38, 5745–5758, https://doi.org/10.1016/j.atmosenv.2004.01.054, 2004.

Allan, J. D., Delia, A. E., Coe, H., Bower, K. N., Alfarra, M. R., Jimenez, J. L., Middlebrook, A. M., Drewnick, F., Onasch, T. B., Canagaratna, M. R., Jayne, J. T., and Worsnop, D. R.: A generalised method for the extraction of chemically resolved mass spectra from Aerodyne aerosol mass spectrometer data, Journal of Aerosol Science, 35, 909–922, https://doi.org/10.1016/j.jaerosci.2004.02.007, 2004.

Allan, J. D., Alfarra, M. R., Bower, K. N., Coe, H., Jayne, J. T., Worsnop, D. R., Aalto, P. P., Kulmala, M., Hyötyläinen, T., Cavalli, F., and Laaksonen, A.: Size and composition measurements of background aerosol and new particle growth in a Finnish forest during QUEST 2 using an Aerodyne Aerosol Mass Spectrometer, Atmospheric Chemistry and Physics, 6, 315–327, https://doi.org/10.5194/acp-6-315-2006, 2006.

484 FLAME: http://chem.atmos.colostate.edu/FLAME/.

485 Aurela, M., Saarikoski, S., Niemi, J. V., Canonaco, F., Prevot, A. S. H., Frey, A., Carbone, S., Kousa, A., and Hillamo, R.:
486 Chemical and Source Characterization of Submicron Particles at Residential and Traffic Sites in the Helsinki Metropolitan
487 Area, Finland, Aerosol Air Qual. Res., 15, 1213–1226, https://doi.org/10.4209/aaqr.2014.11.0279, 2015.

488 Bahreini, R., Jimenez, J. L., Wang, J., Flagan, R. C., Seinfeld, J. H., Jayne, J. T., and Worsnop, D. R.: Aircraft-based aerosol
489 size and composition measurements during ACE-Asia using an Aerodyne aerosol mass spectrometer, Journal of Geophysical
490 Research: Atmospheres, 108, https://doi.org/10.1029/2002JD003226, 2003.

491 Bahreini, R., Keywood, M. D., Ng, N. L., Varutbangkul, V., Gao, S., Flagan, R. C., Seinfeld, J. H., Worsnop, D. R., and
492 Jimenez, J. L.: Measurements of Secondary Organic Aerosol from Oxidation of Cycloalkenes, Terpenes, and m-Xylene
493 Using an Aerodyne Aerosol Mass Spectrometer, Environ. Sci. Technol., 39, 5674–5688, https://doi.org/10.1021/es048061a,
494 2005.

495 Baltensperger, U., Chirico, R., DeCarlo, P. F., Dommen, J., Gaeggeler, K., Heringa, M. F., Li, M., Prévôt, A. S. H., Alfarra,
496 M. R., Gross, D. S., and Kalberer, M.: Recent Developments in the Mass Spectrometry of Atmospheric Aerosols, Eur J Mass
497 Spectrom (Chichester), 16, 389–395, https://doi.org/10.1255/ejms.1084, 2010.

498 Bates, T. S., Quinn, P. K., Frossard, A. A., Russell, L. M., Hakala, J., Petäjä, T., Kulmala, M., Covert, D. S., Cappa, C. D.,
499 Li, S.-M., Hayden, K. L., Nuaaman, I., McLaren, R., Massoli, P., Canagaratna, M. R., Onasch, T. B., Sueper, D., Worsnop,
500 D. R., and Keene, W. C.: Measurements of ocean derived aerosol off the coast of California, Journal of Geophysical
501 Research: Atmospheres, 117, https://doi.org/10.1029/2012JD017588, 2012.

502 Bäumer, D., Vogel, B., Versick, S., Rinke, R., Möhler, O., and Schnaiter, M.: Relationship of visibility, aerosol optical
503 thickness and aerosol size distribution in an ageing air mass over South-West Germany, Atmospheric Environment, 42, 989–
504 998, https://doi.org/10.1016/j.atmosenv.2007.10.017, 2008.

505 Boyd, C. M., Nah, T., Xu, L., Berkemeier, T., and Ng, N. L.: Secondary Organic Aerosol (SOA) from Nitrate Radical
506 Oxidation of Monoterpenes: Effects of Temperature, Dilution, and Humidity on Aerosol Formation, Mixing, and
507 Evaporation, Environ. Sci. Technol., 51, 7831–7841, https://doi.org/10.1021/acs.est.7b01460, 2017.

508 Bressi, M., Cavalli, F., Belis, C. A., Putaud, J.-P., Fröhlich, R., Martins dos Santos, S., Petralia, E., Prévôt, A. S. H., Berico,
509 M., Malaguti, A., and Canonaco, F.: Variations in the chemical composition of the submicron aerosol and in the sources of
510 the organic fraction at a regional background site of the Po Valley (Italy), Atmospheric Chemistry and Physics, 16, 12875–
511 12896, https://doi.org/10.5194/acp-16-12875-2016, 2016.

512 Budisulistiorini, S. H., Canagaratna, M. R., Croteau, P. L., Marth, W. J., Baumann, K., Edgerton, E. S., Shaw, S. L.,
513 Knipping, E. M., Worsnop, D. R., Jayne, J. T., Gold, A., and Surratt, J. D.: Real-Time Continuous Characterization of
514 Secondary Organic Aerosol Derived from Isoprene Epoxydiols in Downtown Atlanta, Georgia, Using the Aerodyne Aerosol
515 Chemical Speciation Monitor, Environ. Sci. Technol., 47, 5686–5694, https://doi.org/10.1021/es400023n, 2013.

516 Budisulistiorini, S. H., Canagaratna, M. R., Croteau, P. L., Baumann, K., Edgerton, E. S., Kollman, M. S., Ng, N. L., Verma,
517 V., Shaw, S. L., Knipping, E. M., Worsnop, D. R., Jayne, J. T., Weber, R. J., and Surratt, J. D.: Intercomparison of an
518 Aerosol Chemical Speciation Monitor (ACSM) with ambient fine aerosol measurements in downtown Atlanta, Georgia,
519 Atmospheric Measurement Techniques, 7, 1929–1941, https://doi.org/10.5194/amt-7-1929-2014, 2014.

520 Budisulistiorini, S. H., Li, X., Bairai, S. T., Renfro, J., Liu, Y., Liu, Y. J., McKinney, K. A., Martin, S. T., McNeill, V. F.,
521 Pye, H. O. T., Nenes, A., Neff, M. E., Stone, E. A., Mueller, S., Knote, C., Shaw, S. L., Zhang, Z., Gold, A., and Surratt, J.
522 D.: Examining the effects of anthropogenic emissions on isoprene-derived secondary organic aerosol formation during the
523 2013 Southern Oxidant and Aerosol Study (SOAS) at the Look Rock, Tennessee ground site, Atmospheric Chemistry and
524 Physics, 15, 8871–8888, https://doi.org/10.5194/acp-15-8871-2015, 2015.

525 Budisulistiorini, S. H., Baumann, K., Edgerton, E. S., Bairai, S. T., Mueller, S., Shaw, S. L., Knipping, E. M., Gold, A., and
526 Surratt, J. D.: Seasonal characterization of submicron aerosol chemical composition and organic aerosol sources in the
527 southeastern United States: Atlanta, Georgia,and Look Rock, Tennessee, Atmospheric Chemistry and Physics, 16, 5171–
528 5189, https://doi.org/10.5194/acp-16-5171-2016, 2016.

529 Canagaratna, M. R., Jayne, J. T., Ghertner, D. A., Herndon, S., Shi, Q., Jimenez, J. L., Silva, P. J., Williams, P., Lanni, T.,
530 Drewnick, F., Demerjian, K. L., Kolb, C. E., and Worsnop, D. R.: Chase Studies of Particulate Emissions from in-use New
531 York City Vehicles, Aerosol Science and Technology, 38, 555–573, https://doi.org/10.1080/02786820490465504, 2004.

Canagaratna, M. r., Jayne, J. t., Jimenez, J. l., Allan, J. d., Alfarra, M. r., Zhang, Q., Onasch, T. b., Drewnick, F., Coe, H., Middlebrook, A., Delia, A., Williams, L. r., Trimborn, A. m., Northway, M. j., DeCarlo, P. f., Kolb, C. e., Davidovits, P., and Worsnop, D. r.: Chemical and microphysical characterization of ambient aerosols with the aerodyne aerosol mass spectrometer, Mass Spectrometry Reviews, 26, 185–222, https://doi.org/10.1002/mas.20115, 2007.

Canonaco, F., Crippa, M., Slowik, J. G., Baltensperger, U., and Prévôt, A. S. H.: SoFi, an IGOR-based interface for the efficient use of the generalized multilinear engine (ME-2) for the source apportionment: ME-2 application to aerosol mass spectrometer data, Atmospheric Measurement Techniques, 6, 3649–3661, https://doi.org/10.5194/amt-6-3649-2013, 2013.

Canonaco, F., Slowik, J. G., Baltensperger, U., and Prévôt, A. S. H.: Seasonal differences in oxygenated organic aerosol composition: implications for emissions sources and factor analysis, Atmospheric Chemistry and Physics, 15, 6993–7002, https://doi.org/10.5194/acp-15-6993-2015, 2015.

Carbone, S., Saarikoski, S., Frey, A., Reyes, F., Reyes, P., Castillo, M., Gramsch, E., Oyola, P., Jayne, J., Worsnop, D. R., and Hillamo, R.: Chemical Characterization of Submicron Aerosol Particles in Santiago de Chile, Aerosol Air Qual. Res., 13, 462–473, https://doi.org/10.4209/aaqr.2012.10.0261, 2013.

Chhabra, P. S., Flagan, R. C., and Seinfeld, J. H.: Elemental analysis of chamber organic aerosol using an aerodyne high-resolution aerosol mass spectrometer, Atmospheric Chemistry and Physics, 10, 4111–4131, https://doi.org/10.5194/acp-10-4111-2010, 2010.

Chirico, R., DeCarlo, P. F., Heringa, M. F., Tritscher, T., Richter, R., Prévôt, A. S. H., Dommen, J., Weingartner, E., Wehrle, G., Gysel, M., Laborde, M., and Baltensperger, U.: Impact of aftertreatment devices on primary emissions and secondary organic aerosol formation potential from in-use diesel vehicles: results from smog chamber experiments, Atmospheric Chemistry and Physics, 10, 11545–11563, https://doi.org/10.5194/acp-10-11545-2010, 2010.

Claeys, M., Roberts, G., Mallet, M., Arndt, J., Sellegri, K., Sciare, J., Wenger, J., and Sauvage, B.: Optical, physical and chemical properties of aerosols transported to a coastal site in the western Mediterranean: a focus on primary marine aerosols, Atmospheric Chemistry and Physics, 17, 7891–7915, https://doi.org/10.5194/acp-17-7891-2017, 2017.

Cleveland, M. J., Ziemba, L. D., Griffin, R. J., Dibb, J. E., Anderson, C. H., Lefer, B., and Rappenglück, B.: Characterization of urban aerosol using aerosol mass spectrometry and proton nuclear magnetic resonance spectroscopy, Atmospheric Environment, 54, 511–518, https://doi.org/10.1016/j.atmosenv.2012.02.074, 2012.

Coggon, M. M., Sorooshian, A., Wang, Z., Metcalf, A. R., Frossard, A. A., Lin, J. J., Craven, J. S., Nenes, A., Jonsson, H. H., Russell, L. M., Flagan, R. C., and Seinfeld, J. H.: Ship impacts on the marine atmosphere: insights into the contribution of shipping emissions to the properties of marine aerosol and clouds, Atmospheric Chemistry and Physics, 12, 8439–8458, https://doi.org/10.5194/acp-12-8439-2012, 2012.

Collier, S., Zhou, S., Kuwayama, T., Forestieri, S., Brady, J., Zhang, M., Kleeman, M., Cappa, C., Bertram, T., and Zhang, Q.: Organic PM Emissions from Vehicles: Composition, O/C Ratio, and Dependence on PM Concentration, Aerosol Science and Technology, 49, 86–97, https://doi.org/10.1080/02786826.2014.1003364, 2015.

Crippa, M., El Haddad, I., Slowik, J. G., DeCarlo, P. F., Mohr, C., Heringa, M. F., Chirico, R., Marchand, N., Sciare, J., Baltensperger, U., and Prévôt, A. S. H.: Identification of marine and continental aerosol sources in Paris using high resolution aerosol mass spectrometry, Journal of Geophysical Research: Atmospheres, 118, 1950–1963, https://doi.org/10.1002/jgrd.50151, 2013.

Dall'Osto, M., Ovadnevaite, J., Ceburnis, D., Martin, D., Healy, R. M., O'Connor, I. P., Kourtchev, I., Sodeau, J. R., Wenger, J. C., and O'Dowd, C.: Characterization of urban aerosol in Cork city (Ireland) using aerosol mass spectrometry, Atmospheric Chemistry and Physics, 13, 4997–5015, https://doi.org/10.5194/acp-13-4997-2013, 2013.

Day, D. A., Fry, J. L., Kang, H. G., Krechmer, J. E., Ayres, B. R., Keehan, N. I., Thompson, S. L., Hu, W., Campuzano-Jost, P., Schroder, J. C., Stark, H., DeVault, M. P., Ziemann, P. J., Zarzana, K. J., Wild, R. J., Dubè, W. P., Brown, S. S., and Jimenez, J. L.: Secondary Organic Aerosol Mass Yields from NO3 Oxidation of α-Pinene and Δ-Carene: Effect of RO2 Radical Fate, J. Phys. Chem. A, 126, 7309–7330, https://doi.org/10.1021/acs.jpca.2c04419, 2022.

De Gouw, J. and Jimenez, J. L.: Organic Aerosols in the Earth's Atmosphere, Environ. Sci. Technol., 43, 7614–7618, https://doi.org/10.1021/es9006004, 2009.

DeCarlo, P. F., Kimmel, J. R., Trimborn, A., Northway, M. J., Jayne, J. T., Aiken, A. C., Gonin, M., Fuhrer, K., Horvath, T., Docherty, K. S., Worsnop, D. R., and Jimenez, J. L.: Field-Deployable, High-Resolution, Time-of-Flight Aerosol Mass Spectrometer, Anal. Chem., 78, 8281–8289, https://doi.org/10.1021/ac061249n, 2006.

Docherty, K. S., Aiken, A. C., Huffman, J. A., Ulbrich, I. M., DeCarlo, P. F., Sueper, D., Worsnop, D. R., Snyder, D. C., Peltier, R. E., Weber, R. J., Grover, B. D., Eatough, D. J., Williams, B. J., Goldstein, A. H., Ziemann, P. J., and Jimenez, J. L.: The 2005 Study of Organic Aerosols at Riverside (SOAR-1): instrumental intercomparisons and fine particle composition, Atmospheric Chemistry and Physics, 11, 12387–12420, https://doi.org/10.5194/acp-11-12387-2011, 2011.

Drewnick, F., Böttger, T., von der Weiden-Reinmüller, S.-L., Zorn, S. R., Klimach, T., Schneider, J., and Borrmann, S.: Design of a mobile aerosol research laboratory and data processing tools for effective stationary and mobile field measurements, Atmospheric Measurement Techniques, 5, 1443–1457, https://doi.org/10.5194/amt-5-1443-2012, 2012.

Elser, M., Huang, R.-J., Wolf, R., Slowik, J. G., Wang, Q., Canonaco, F., Li, G., Bozzetti, C., Daellenbach, K. R., Huang, Y., Zhang, R., Li, Z., Cao, J., Baltensperger, U., El-Haddad, I., and Prévôt, A. S. H.: New insights into $PM_{2.5}$ chemical composition and sources in two major cities in China during extreme haze events using aerosol mass spectrometry, Atmospheric Chemistry and Physics, 16, 3207–3225, https://doi.org/10.5194/acp-16-3207-2016, 2016.

Fortenberry, C. F., Walker, M. J., Zhang, Y., Mitroo, D., Brune, W. H., and Williams, B. J.: Bulk and molecular-level characterization of laboratory-aged biomass burning organic aerosol from oak leaf and heartwood fuels, Atmospheric Chemistry and Physics, 18, 2199–2224, https://doi.org/10.5194/acp-18-2199-2018, 2018.

Fröhlich, R., Cubison, M. J., Slowik, J. G., Bukowiecki, N., Prévôt, A. S. H., Baltensperger, U., Schneider, J., Kimmel, J. R., Gonin, M., Rohner, U., Worsnop, D. R., and Jayne, J. T.: The ToF-ACSM: a portable aerosol chemical speciation monitor with TOFMS detection, Atmospheric Measurement Techniques, 6, 3225–3241, https://doi.org/10.5194/amt-6-3225-2013, 2013.

Fröhlich, R., Crenn, V., Setyan, A., Belis, C. A., Canonaco, F., Favez, O., Riffault, V., Slowik, J. G., Aas, W., Aijälä, M., Alastuey, A., Artiñano, B., Bonnaire, N., Bozzetti, C., Bressi, M., Carbone, C., Coz, E., Croteau, P. L., Cubison, M. J., Esser-Gietl, J. K., Green, D. C., Gros, V., Heikkinen, L., Herrmann, H., Jayne, J. T., Lunder, C. R., Minguillón, M. C., Močnik, G., O'Dowd, C. D., Ovadnevaite, J., Petralia, E., Poulain, L., Priestman, M., Ripoll, A., Sarda-Estève, R., Wiedensohler, A., Baltensperger, U., Sciare, J., and Prévôt, A. S. H.: ACTRIS ACSM intercomparison – Part 2: Intercomparison of ME-2 organic source apportionment results from 15 individual, co-located aerosol mass spectrometers, Atmospheric Measurement Techniques, 8, 2555–2576, https://doi.org/10.5194/amt-8-2555-2015, 2015a.

Fröhlich, R., Cubison, M. J., Slowik, J. G., Bukowiecki, N., Canonaco, F., Croteau, P. L., Gysel, M., Henne, S., Herrmann, E., Jayne, J. T., Steinbacher, M., Worsnop, D. R., Baltensperger, U., and Prévôt, A. S. H.: Fourteen months of on-line measurements of the non-refractory submicron aerosol at the Jungfraujoch (3580 m a.s.l.) – chemical composition, origins and organic aerosol sources, Atmospheric Chemistry and Physics, 15, 11373–11398, https://doi.org/10.5194/acp-15-11373-2015, 2015b.

Goldstein, A. H. and Galbally, I. E.: Known and unexplored organic constituents in the earth's atmosphere, Environmental science & technology, 41, 1514–1521, 2007.

Hao, L. Q., Kortelainen, A., Romakkaniemi, S., Portin, H., Jaatinen, A., Leskinen, A., Komppula, M., Miettinen, P., Sueper, D., Pajunoja, A., Smith, J. N., Lehtinen, K. E. J., Worsnop, D. R., Laaksonen, A., and Virtanen, A.: Atmospheric submicron aerosol composition and particulate organic nitrate formation in a boreal forestland–urban mixed region, Atmospheric Chemistry and Physics, 14, 13483–13495, https://doi.org/10.5194/acp-14-13483-2014, 2014.

Hayes, P. L., Ortega, A. M., Cubison, M. J., Froyd, K. D., Zhao, Y., Cliff, S. S., Hu, W. W., Toohey, D. W., Flynn, J. H., Lefer, B. L., Grossberg, N., Alvarez, S., Rappenglück, B., Taylor, J. W., Allan, J. D., Holloway, J. S., Gilman, J. B., Kuster, W. C., de Gouw, J. A., Massoli, P., Zhang, X., Liu, J., Weber, R. J., Corrigan, A. L., Russell, L. M., Isaacman, G., Worton, D. R., Kreisberg, N. M., Goldstein, A. H., Thalman, R., Waxman, E. M., Volkamer, R., Lin, Y. H., Surratt, J. D., Kleindienst, T. E., Offenberg, J. H., Dusanter, S., Griffith, S., Stevens, P. S., Brioude, J., Angevine, W. M., and Jimenez, J. L.: Organic aerosol composition and sources in Pasadena, California, during the 2010 CalNex campaign, Journal of Geophysical Research: Atmospheres, 118, 9233–9257, https://doi.org/10.1002/jgrd.50530, 2013.

He, L.-Y., Lin, Y., Huang, X.-F., Guo, S., Xue, L., Su, Q., Hu, M., Luan, S.-J., and Zhang, Y.-H.: Characterization of high-resolution aerosol mass spectra of primary organic aerosol emissions from Chinese cooking and biomass burning, Atmospheric Chemistry and Physics, 10, 11535–11543, https://doi.org/10.5194/acp-10-11535-2010, 2010.

He, L.-Y., Huang, X.-F., Xue, L., Hu, M., Lin, Y., Zheng, J., Zhang, R., and Zhang, Y.-H.: Submicron aerosol analysis and organic source apportionment in an urban atmosphere in Pearl River Delta of China using high-resolution aerosol mass spectrometry, Journal of Geophysical Research: Atmospheres, 116, https://doi.org/10.1029/2010JD014566, 2011.

Heikkinen, L., Äijälä, M., Riva, M., Luoma, K., Dällenbach, K., Aalto, J., Aalto, P., Aliaga, D., Aurela, M., Keskinen, H., Makkonen, U., Rantala, P., Kulmala, M., Petäjä, T., Worsnop, D., and Ehn, M.: Long-term sub-micrometer aerosol chemical composition in the boreal forest: inter- and intra-annual variability, Atmospheric Chemistry and Physics, 20, 3151–3180, https://doi.org/10.5194/acp-20-3151-2020, 2020.

Heringa, M. F., DeCarlo, P. F., Chirico, R., Tritscher, T., Dommen, J., Weingartner, E., Richter, R., Wehrle, G., Prévôt, A. S. H., and Baltensperger, U.: Investigations of primary and secondary particulate matter of different wood combustion appliances with a high-resolution time-of-flight aerosol mass spectrometer, Atmospheric Chemistry and Physics, 11, 5945–5957, https://doi.org/10.5194/acp-11-5945-2011, 2011.

Hu, W., Hu, M., Hu, W., Jimenez, J. L., Yuan, B., Chen, W., Wang, M., Wu, Y., Chen, C., Wang, Z., Peng, J., Zeng, L., and Shao, M.: Chemical composition, sources, and aging process of submicron aerosols in Beijing: Contrast between summer and winter, Journal of Geophysical Research: Atmospheres, 121, 1955–1977, https://doi.org/10.1002/2015JD024020, 2016.

Hu, W., Day, D. A., Campuzano-Jost, P., Nault, B. A., Park, T., Lee, T., Croteau, P., Canagaratna, M. R., Jayne, J. T., Worsnop, D. R., and Jimenez, J. L.: Evaluation of the New Capture Vaporizer for Aerosol Mass Spectrometers (AMS): Elemental Composition and Source Apportionment of Organic Aerosols (OA), ACS Earth Space Chem., 2, 410–421, https://doi.org/10.1021/acsearthspacechem.8b00002, 2018a.

Hu, W., Day, D. A., Campuzano-Jost, P., Nault, B. A., Park, T., Lee, T., Croteau, P., Canagaratna, M. R., Jayne, J. T., Worsnop, D. R., and Jimenez, J. L.: Evaluation of the new capture vaporizer for aerosol mass spectrometers: Characterization of organic aerosol mass spectra, Aerosol Science and Technology, 52, 725–739, https://doi.org/10.1080/02786826.2018.1454584, 2018b.

Hu, W. W., Hu, M., Yuan, B., Jimenez, J. L., Tang, Q., Peng, J. F., Hu, W., Shao, M., Wang, M., Zeng, L. M., Wu, Y. S., Gong, Z. H., Huang, X. F., and He, L. Y.: Insights on organic aerosol aging and the influence of coal combustion at a regional receptor site of central eastern China, Atmospheric Chemistry and Physics, 13, 10095–10112, https://doi.org/10.5194/acp-13-10095-2013, 2013.

Hu, W. W., Campuzano-Jost, P., Palm, B. B., Day, D. A., Ortega, A. M., Hayes, P. L., Krechmer, J. E., Chen, Q., Kuwata, M., Liu, Y. J., de Sá, S. S., McKinney, K., Martin, S. T., Hu, M., Budisulistiorini, S. H., Riva, M., Surratt, J. D., St. Clair, J. M., Isaacman-Van Wertz, G., Yee, L. D., Goldstein, A. H., Carbone, S., Brito, J., Artaxo, P., de Gouw, J. A., Koss, A., Wisthaler, A., Mikoviny, T., Karl, T., Kaser, L., Jud, W., Hansel, A., Docherty, K. S., Alexander, M. L., Robinson, N. H., Coe, H., Allan, J. D., Canagaratna, M. R., Paulot, F., and Jimenez, J. L.: Characterization of a real-time tracer for isoprene epoxydiols-derived secondary organic aerosol (IEPOX-SOA) from aerosol mass spectrometer measurements, Atmospheric Chemistry and Physics, 15, 11807–11833, https://doi.org/10.5194/acp-15-11807-2015, 2015.

IPCC: Climate Change 2021: The Physical Science Basis. Contribution of Working Group I to the Sixth Assessment Report of the Intergovernmental Panel on Climate Change, , In Press, https://doi.org/10.1017/9781009157896, 2021.

Jayne, J. T., Leard, D. C., Zhang, X., Davidovits, P., Smith, K. A., Kolb, C. E., and Worsnop, D. R.: Development of an Aerosol Mass Spectrometer for Size and Composition Analysis of Submicron Particles, Aerosol Science and Technology, 33, 49–70, https://doi.org/10.1080/027868200410840, 2000.

Jimenez, J. L., Jayne, J. T., Shi, Q., Kolb, C. E., Worsnop, D. R., Yourshaw, I., Seinfeld, J. H., Flagan, R. C., Zhang, X., Smith, K. A., Morris, J. W., and Davidovits, P.: Ambient aerosol sampling using the Aerodyne Aerosol Mass Spectrometer, Journal of Geophysical Research: Atmospheres, 108, https://doi.org/10.1029/2001JD001213, 2003.

Kampa, M. and Castanas, E.: Human health effects of air pollution, Environmental Pollution, 151, 362–367, https://doi.org/10.1016/j.envpol.2007.06.012, 2008.

Katrib, Y., Martin, S. T., Hung, H.-M., Rudich, Y., Zhang, H., Slowik, J. G., Davidovits, P., Jayne, J. T., and Worsnop, D. R.: Products and Mechanisms of Ozone Reactions with Oleic Acid for Aerosol Particles Having Core−Shell Morphologies, J. Phys. Chem. A, 108, 6686–6695, https://doi.org/10.1021/jp049759d, 2004.

Kim, H., Zhang, Q., Bae, G.-N., Kim, J. Y., and Lee, S. B.: Sources and atmospheric processing of winter aerosols in Seoul, Korea: insights from real-time measurements using a high-resolution aerosol mass spectrometer, Atmospheric Chemistry and

675 Physics, 17, 2009–2033, https://doi.org/10.5194/acp-17-2009-2017, 2017.

676 Kommula, S. M., Upasana, P., Sharma, A., Raj, S. S., Reyes-villegas, E., Liu, T., Allan, J. D., Jose, C., Pöhlker, M. L.,
677 Ravikrishna, R., Liu, P., Su, H., Martin, S. T., Pöschl, U., Mcfiggans, G., Coe, H., and Gunthe, S. S.: Chemical
678 Characterization and Source Apportionment of Organic Aerosols in the Coastal City of Chennai, India: Impact of Marine Air
679 Masses on Aerosol Chemical Composition and Potential for Secondary Organic Aerosol Formation, ACS Earth Space
680 Chem., 5, 3197–3209, https://doi.org/10.1021/acsearthspacechem.1c00276, 2021.

681 Kroll, J. H., Ng, N. L., Murphy, S. M., Flagan, R. C., and Seinfeld, J. H.: Secondary organic aerosol formation from isoprene
682 photooxidation under high-NOx conditions, Geophysical Research Letters, 32, https://doi.org/10.1029/2005GL023637, 2005.

683 Kroll, J. H., Ng, N. L., Murphy, S. M., Flagan, R. C., and Seinfeld, J. H.: Secondary Organic Aerosol Formation from
684 Isoprene Photooxidation, Environ. Sci. Technol., 40, 1869–1877, https://doi.org/10.1021/es0524301, 2006.

685 Lambe, A. T., Onasch, T. B., Massoli, P., Croasdale, D. R., Wright, J. P., Ahern, A. T., Williams, L. R., Worsnop, D. R.,
686 Brune, W. H., and Davidovits, P.: Laboratory studies of the chemical composition and cloud condensation nuclei (CCN)
687 activity of secondary organic aerosol (SOA) and oxidized primary organic aerosol (OPOA), Atmospheric Chemistry and
688 Physics, 11, 8913–8928, https://doi.org/10.5194/acp-11-8913-2011, 2011.

689 Lambe, A. T., Onasch, T. B., Croasdale, D. R., Wright, J. P., Martin, A. T., Franklin, J. P., Massoli, P., Kroll, J. H.,
690 Canagaratna, M. R., Brune, W. H., Worsnop, D. R., and Davidovits, P.: Transitions from Functionalization to Fragmentation
691 Reactions of Laboratory Secondary Organic Aerosol (SOA) Generated from the OH Oxidation of Alkane Precursors,
692 Environ. Sci. Technol., 46, 5430–5437, https://doi.org/10.1021/es300274t, 2012.

693 Lambe, A. T., Chhabra, P. S., Onasch, T. B., Brune, W. H., Hunter, J. F., Kroll, J. H., Cummings, M. J., Brogan, J. F.,
694 Parmar, Y., Worsnop, D. R., Kolb, C. E., and Davidovits, P.: Effect of oxidant concentration, exposure time, and seed
695 particles on secondary organic aerosol chemical composition and yield, Atmos. Chem. Phys., 15, 3063–3075,
696 https://doi.org/10.5194/acp-15-3063-2015, 2015.

697 Lanz, V. A., Alfarra, M. R., Baltensperger, U., Buchmann, B., Hueglin, C., and Prévôt, A. S. H.: Source apportionment of
698 submicron organic aerosols at an urban site by factor analytical modelling of aerosol mass spectra, Atmospheric Chemistry
699 and Physics, 7, 1503–1522, https://doi.org/10.5194/acp-7-1503-2007, 2007.

700 Lee, T., Choi, J., Lee, G., Ahn, J., Park, J. S., Atwood, S. A., Schurman, M., Choi, Y., Chung, Y., and Collett, J. L.:
701 Characterization of aerosol composition, concentrations, and sources at Baengnyeong Island, Korea using an aerosol mass
702 spectrometer, Atmospheric Environment, 120, 297–306, https://doi.org/10.1016/j.atmosenv.2015.08.038, 2015.

703 Li, Y. J., Yeung, J. W. T., Leung, T. P. I., Lau, A. P. S., and Chan, C. K.: Characterization of Organic Particles from Incense
704 Burning Using an Aerodyne High-Resolution Time-of-Flight Aerosol Mass Spectrometer, Aerosol Science and Technology,
705 46, 654–665, https://doi.org/10.1080/02786826.2011.653017, 2012.

706 Lim, C. Y., Hagan, D. H., Coggon, M. M., Koss, A. R., Sekimoto, K., de Gouw, J., Warneke, C., Cappa, C. D., and Kroll, J.
707 H.: Secondary organic aerosol formation from the laboratory oxidation of biomass burning emissions, Atmospheric
708 Chemistry and Physics, 19, 12797–12809, https://doi.org/10.5194/acp-19-12797-2019, 2019.

709 Loza, C. L., Chhabra, P. S., Yee, L. D., Craven, J. S., Flagan, R. C., and Seinfeld, J. H.: Chemical aging of *m*-xylene
710 secondary organic aerosol: laboratory chamber study, Atmospheric Chemistry and Physics, 12, 151–167,
711 https://doi.org/10.5194/acp-12-151-2012, 2012.

712 Loza, C. L., Craven, J. S., Yee, L. D., Coggon, M. M., Schwantes, R. H., Shiraiwa, M., Zhang, X., Schilling, K. A., Ng, N.
713 L., Canagaratna, M. R., Ziemann, P. J., Flagan, R. C., and Seinfeld, J. H.: Secondary organic aerosol yields of 12-carbon
714 alkanes, Atmospheric Chemistry and Physics, 14, 1423–1439, https://doi.org/10.5194/acp-14-1423-2014, 2014.

715 Marcolli, C., Canagaratna, M. R., Worsnop, D. R., Bahreini, R., de Gouw, J. A., Warneke, C., Goldan, P. D., Kuster, W. C.,
716 Williams, E. J., Lerner, B. M., Roberts, J. M., Meagher, J. F., Fehsenfeld, F. C., Marchewka, M., Bertman, S. B., and
717 Middlebrook, A. M.: Cluster Analysis of the Organic Peaks in Bulk Mass Spectra Obtained During the 2002 New England
718 Air Quality Study with an Aerodyne Aerosol Mass Spectrometer, Atmospheric Chemistry and Physics, 6, 5649–5666,
719 https://doi.org/10.5194/acp-6-5649-2006, 2006.

720 Michoud, V., Sciare, J., Sauvage, S., Dusanter, S., Léonardis, T., Gros, V., Kalogridis, C., Zannoni, N., Féron, A., Petit, J.-E.,
721 Crenn, V., Baisnée, D., Sarda-Estève, R., Bonnaire, N., Marchand, N., DeWitt, H. L., Pey, J., Colomb, A., Gheusi, F., Szidat,

S., Stavroulas, I., Borbon, A., and Locoge, N.: Organic carbon at a remote site of the western Mediterranean Basin: sources and chemistry during the ChArMEx SOP2 field experiment, Atmospheric Chemistry and Physics, 17, 8837–8865, https://doi.org/10.5194/acp-17-8837-2017, 2017.

Minguillón, M. C., Perron, N., Querol, X., Szidat, S., Fahrni, S. M., Alastuey, A., Jimenez, J. L., Mohr, C., Ortega, A. M., Day, D. A., Lanz, V. A., Wacker, L., Reche, C., Cusack, M., Amato, F., Kiss, G., Hoffer, A., Decesari, S., Moretti, F., Hillamo, R., Teinilä, K., Seco, R., Peñuelas, J., Metzger, A., Schallhart, S., Müller, M., Hansel, A., Burkhart, J. F., Baltensperger, U., and Prévôt, A. S. H.: Fossil versus contemporary sources of fine elemental and organic carbonaceous particulate matter during the DAURE campaign in Northeast Spain, Atmospheric Chemistry and Physics, 11, 12067–12084, https://doi.org/10.5194/acp-11-12067-2011, 2011.

Minguillón, M. C., Ripoll, A., Pérez, N., Prévôt, A. S. H., Canonaco, F., Querol, X., and Alastuey, A.: Chemical characterization of submicron regional background aerosols in the western Mediterranean using an Aerosol Chemical Speciation Monitor, Atmospheric Chemistry and Physics, 15, 6379–6391, https://doi.org/10.5194/acp-15-6379-2015, 2015.

Modini, R. L., Frossard, A. A., Ahlm, L., Russell, L. M., Corrigan, C. E., Roberts, G. C., Hawkins, L. N., Schroder, J. C., Bertram, A. K., Zhao, R., Lee, A. K. Y., Abbatt, J. P. D., Lin, J., Nenes, A., Wang, Z., Wonaschütz, A., Sorooshian, A., Noone, K. J., Jonsson, H., Seinfeld, J. H., Toom-Sauntry, D., Macdonald, A. M., and Leaitch, W. R.: Primary marine aerosol-cloud interactions off the coast of California, Journal of Geophysical Research: Atmospheres, 120, 4282–4303, https://doi.org/10.1002/2014JD022963, 2015.

Mohr, C., Huffman, J. A., Cubison, M. J., Aiken, A. C., Docherty, K. S., Kimmel, J. R., Ulbrich, I. M., Hannigan, M., and Jimenez, J. L.: Characterization of Primary Organic Aerosol Emissions from Meat Cooking, Trash Burning, and Motor Vehicles with High-Resolution Aerosol Mass Spectrometry and Comparison with Ambient and Chamber Observations, Environ. Sci. Technol., 43, 2443–2449, https://doi.org/10.1021/es8011518, 2009.

Mohr, C., Richter, R., DeCarlo, P. F., Prévôt, A. S. H., and Baltensperger, U.: Spatial variation of chemical composition and sources of submicron aerosol in Zurich during wintertime using mobile aerosol mass spectrometer data, Atmospheric Chemistry and Physics, 11, 7465–7482, https://doi.org/10.5194/acp-11-7465-2011, 2011.

Mohr, C., DeCarlo, P. F., Heringa, M. F., Chirico, R., Slowik, J. G., Richter, R., Reche, C., Alastuey, A., Querol, X., Seco, R., Peñuelas, J., Jiménez, J. L., Crippa, M., Zimmermann, R., Baltensperger, U., and Prévôt, A. S. H.: Identification and quantification of organic aerosol from cooking and other sources in Barcelona using aerosol mass spectrometer data, Atmospheric Chemistry and Physics, 12, 1649–1665, https://doi.org/10.5194/acp-12-1649-2012, 2012.

Murphy, S. M., Sorooshian, A., Kroll, J. H., Ng, N. L., Chhabra, P., Tong, C., Surratt, J. D., Knipping, E., Flagan, R. C., and Seinfeld, J. H.: Secondary aerosol formation from atmospheric reactions of aliphatic amines, Atmospheric Chemistry and Physics, 7, 2313–2337, https://doi.org/10.5194/acp-7-2313-2007, 2007.

Ng, N. L., Chhabra, P. S., Chan, A. W. H., Surratt, J. D., Kroll, J. H., Kwan, A. J., McCabe, D. C., Wennberg, P. O., Sorooshian, A., Murphy, S. M., Dalleska, N. F., Flagan, R. C., and Seinfeld, J. H.: Effect of NO_x level on secondary organic aerosol (SOA) formation from the photooxidation of terpenes, Atmospheric Chemistry and Physics, 7, 5159–5174, https://doi.org/10.5194/acp-7-5159-2007, 2007.

Ng, N. L., Kwan, A. J., Surratt, J. D., Chan, A. W. H., Chhabra, P. S., Sorooshian, A., Pye, H. O. T., Crounse, J. D., Wennberg, P. O., Flagan, R. C., and Seinfeld, J. H.: Secondary organic aerosol (SOA) formation from reaction of isoprene with nitrate radicals (NO_3), Atmospheric Chemistry and Physics, 8, 4117–4140, https://doi.org/10.5194/acp-8-4117-2008, 2008.

Ng, N. L., Herndon, S. C., Trimborn, A., Canagaratna, M. R., Croteau, P. L., Onasch, T. B., Sueper, D., Worsnop, D. R., Zhang, Q., Sun, Y. L., and Jayne, J. T.: An Aerosol Chemical Speciation Monitor (ACSM) for Routine Monitoring of the Composition and Mass Concentrations of Ambient Aerosol, Aerosol Science and Technology, 45, 780–794, https://doi.org/10.1080/02786826.2011.560211, 2011.

Nguyen, T. B., Bates, K. H., Buenconsejo, R. S., Charan, S. M., Cavanna, E. E., Cocker, D. R. I., Day, D. A., DeVault, M. P., Donahue, N. M., Finewax, Z., Habib, L. F., Handschy, A. V., Hildebrandt Ruiz, L., Hou, C.-Y. S., Jimenez, J. L., Joo, T., Klodt, A. L., Kong, W., Le, C., Masoud, C. G., Mayernik, M. S., Ng, N. L., Nienhouse, E. J., Nizkorodov, S. A., Orlando, J. J., Post, J. J., Sturm, P. O., Thrasher, B. L., Tyndall, G. S., Seinfeld, J. H., Worley, S. J., Zhang, X., and Ziemann, P. J.: Overview of ICARUS─A Curated, Open Access, Online Repository for Atmospheric Simulation Chamber Data, ACS Earth Space Chem., 7, 1235–1246, https://doi.org/10.1021/acsearthspacechem.3c00043, 2023.

Paatero, P. and Tapper, U.: Positive matrix factorization: A non-negative factor model with optimal utilization of error estimates of data values, Environmetrics, 5, 111–126, https://doi.org/10.1002/env.3170050203, 1994.

Pandolfi, M., Querol, X., Alastuey, A., Jimenez, J. L., Jorba, O., Day, D., Ortega, A., Cubison, M. J., Comerón, A., Sicard, M., Mohr, C., Prévôt, A. S. H., Minguillón, M. C., Pey, J., Baldasano, J. M., Burkhart, J. F., Seco, R., Peñuelas, J., van Drooge, B. L., Artiñano, B., Di Marco, C., Nemitz, E., Schallhart, S., Metzger, A., Hansel, A., Lorente, J., Ng, S., Jayne, J., and Szidat, S.: Effects of sources and meteorology on particulate matter in the Western Mediterranean Basin: An overview of the DAURE campaign, Journal of Geophysical Research: Atmospheres, 119, 4978–5010, https://doi.org/10.1002/2013JD021079, 2014.

Parworth, C., Fast, J., Mei, F., Shippert, T., Sivaraman, C., Tilp, A., Watson, T., and Zhang, Q.: Long-term measurements of submicrometer aerosol chemistry at the Southern Great Plains (SGP) using an Aerosol Chemical Speciation Monitor (ACSM), Atmospheric Environment, 106, 43–55, https://doi.org/10.1016/j.atmosenv.2015.01.060, 2015.

Pernigotti, D., Belis, C. A., and Spanò, L.: SPECIEUROPE: The European data base for PM source profiles, Atmospheric Pollution Research, 7, 307–314, https://doi.org/10.1016/j.apr.2015.10.007, 2016.

Petit, J.-E., Favez, O., Sciare, J., Crenn, V., Sarda-Estève, R., Bonnaire, N., Močnik, G., Dupont, J.-C., Haeffelin, M., and Leoz-Garziandia, E.: Two years of near real-time chemical composition of submicron aerosols in the region of Paris using an Aerosol Chemical Speciation Monitor (ACSM) and a multi-wavelength Aethalometer, Atmospheric Chemistry and Physics, 15, 2985–3005, https://doi.org/10.5194/acp-15-2985-2015, 2015.

Phinney, L., Richard Leaitch, W., Lohmann, U., Boudries, H., Worsnop, D. R., Jayne, J. T., Toom-Sauntry, D., Wadleigh, M., Sharma, S., and Shantz, N.: Characterization of the aerosol over the sub-arctic north east Pacific Ocean, Deep Sea Research Part II: Topical Studies in Oceanography, 53, 2410–2433, https://doi.org/10.1016/j.dsr2.2006.05.044, 2006.

Pirjola, L., Niemi, J. V., Saarikoski, S., Aurela, M., Enroth, J., Carbone, S., Saarnio, K., Kuuluvainen, H., Kousa, A., Rönkkö, T., and Hillamo, R.: Physical and chemical characterization of urban winter-time aerosols by mobile measurements in Helsinki, Finland, Atmospheric Environment, 158, 60–75, https://doi.org/10.1016/j.atmosenv.2017.03.028, 2017.

Ramanathan, V., Crutzen, P. J., Kiehl, J. T., and Rosenfeld, D.: Aerosols, Climate, and the Hydrological Cycle, Science, 294, 2119–2124, https://doi.org/10.1126/science.1064034, 2001.

Rattanavaraha, W., Canagaratna, M. R., Budisulistiorini, S. H., Croteau, P. L., Baumann, K., Canonaco, F., Prevot, A. S. H., Edgerton, E. S., Zhang, Z., Jayne, J. T., Worsnop, D. R., Gold, A., Shaw, S. L., and Surratt, J. D.: Source apportionment of submicron organic aerosol collected from Atlanta, Georgia, during 2014–2015 using the aerosol chemical speciation monitor (ACSM), Atmospheric Environment, 167, 389–402, https://doi.org/10.1016/j.atmosenv.2017.07.055, 2017.

Reyes-Villegas, E., Green, D. C., Priestman, M., Canonaco, F., Coe, H., Prévôt, A. S. H., and Allan, J. D.: Organic aerosol source apportionment in London 2013 with ME-2: exploring the solution space with annual and seasonal analysis, Atmospheric Chemistry and Physics, 16, 15545–15559, https://doi.org/10.5194/acp-16-15545-2016, 2016.

Ripoll, A., Minguillón, M. C., Pey, J., Jimenez, J. L., Day, D. A., Sosedova, Y., Canonaco, F., Prévôt, A. S. H., Querol, X., and Alastuey, A.: Long-term real-time chemical characterization of submicron aerosols at Montsec (southern Pyrenees, 1570 m a.s.l.), Atmospheric Chemistry and Physics, 15, 2935–2951, https://doi.org/10.5194/acp-15-2935-2015, 2015.

Riva, M., Budisulistiorini, S. H., Chen, Y., Zhang, Z., D'Ambro, E. L., Zhang, X., Gold, A., Turpin, B. J., Thornton, J. A., Canagaratna, M. R., and Surratt, J. D.: Chemical Characterization of Secondary Organic Aerosol from Oxidation of Isoprene Hydroxyhydroperoxides, Environ. Sci. Technol., 50, 9889–9899, https://doi.org/10.1021/acs.est.6b02511, 2016.

Robinson, E. S., Gu, P., Ye, Q., Li, H. Z., Shah, R. U., Apte, J. S., Robinson, A. L., and Presto, A. A.: Restaurant Impacts on Outdoor Air Quality: Elevated Organic Aerosol Mass from Restaurant Cooking with Neighborhood-Scale Plume Extents, Environ. Sci. Technol., 52, 9285–9294, https://doi.org/10.1021/acs.est.8b02654, 2018.

Saarikoski, S., Carbone, S., Decesari, S., Giulianelli, L., Angelini, F., Canagaratna, M., Ng, N. L., Trimborn, A., Facchini, M. C., Fuzzi, S., Hillamo, R., and Worsnop, D.: Chemical characterization of springtime submicrometer aerosol in Po Valley, Italy, Atmospheric Chemistry and Physics, 12, 8401–8421, https://doi.org/10.5194/acp-12-8401-2012, 2012.

Sage, A. M., Weitkamp, E. A., Robinson, A. L., and Donahue, N. M.: Evolving mass spectra of the oxidized component of organic aerosol: results from aerosol mass spectrometer analyses of aged diesel emissions, Atmospheric Chemistry and

817   Physics, 8, 1139–1152, https://doi.org/10.5194/acp-8-1139-2008, 2008.

818   Schlag, P., Kiendler-Scharr, A., Blom, M. J., Canonaco, F., Henzing, J. S., Moerman, M., Prévôt, A. S. H., and Holzinger, R.:
819   Aerosol source apportionment from 1-year measurements at the CESAR tower in Cabauw, the Netherlands, Atmospheric
820   Chemistry and Physics, 16, 8831–8847, https://doi.org/10.5194/acp-16-8831-2016, 2016.

821   Schneider, J., Weimer, S., Drewnick, F., Borrmann, S., Helas, G., Gwaze, P., Schmid, O., Andreae, M. O., and Kirchner, U.:
822   Mass spectrometric analysis and aerodynamic properties of various types of combustion-related aerosol particles,
823   International Journal of Mass Spectrometry, 258, 37–49, https://doi.org/10.1016/j.ijms.2006.07.008, 2006.

824   Setyan, A., Zhang, Q., Merkel, M., Knighton, W. B., Sun, Y., Song, C., Shilling, J. E., Onasch, T. B., Herndon, S. C.,
825   Worsnop, D. R., Fast, J. D., Zaveri, R. A., Berg, L. K., Wiedensohler, A., Flowers, B. A., Dubey, M. K., and Subramanian,
826   R.: Characterization of submicron particles influenced by mixed biogenic and anthropogenic emissions using high-resolution
827   aerosol mass spectrometry: results from CARES, Atmospheric Chemistry and Physics, 12, 8131–8156,
828   https://doi.org/10.5194/acp-12-8131-2012, 2012.

829   Shilling, J. E., Pekour, M. S., Fortner, E. C., Artaxo, P., de Sá, S., Hubbe, J. M., Longo, K. M., Machado, L. A. T., Martin, S.
830   T., Springston, S. R., Tomlinson, J., and Wang, J.: Aircraft observations of the chemical composition and aging of aerosol in
831   the Manaus urban plume during GoAmazon 2014/5, Atmospheric Chemistry and Physics, 18, 10773–10797,
832   https://doi.org/10.5194/acp-18-10773-2018, 2018.

833   Stein, S. E. and Scott, D. R.: Optimization and testing of mass spectral library search algorithms for compound identification,
834   J. Am. Soc. Spectrom., 5, 859–866, https://doi.org/10.1016/1044-0305(94)87009-8, 1994.

835   Struckmeier, C., Drewnick, F., Fachinger, F., Gobbi, G. P., and Borrmann, S.: Atmospheric aerosols in Rome, Italy: sources,
836   dynamics and spatial variations during two seasons, Atmospheric Chemistry and Physics, 16, 15277–15299,
837   https://doi.org/10.5194/acp-16-15277-2016, 2016.

838   Sueper: https://cires1.colorado.edu/jimenez-group/ToFAMSResources/ToFSoftware/, last access: 17 January 2021.

839   Sun, Y., Xu, W., Zhang, Q., Jiang, Q., Canonaco, F., Prévôt, A. S. H., Fu, P., Li, J., Jayne, J., Worsnop, D. R., and Wang, Z.:
840   Source apportionment of organic aerosol from 2-year highly time-resolved measurements by an aerosol chemical speciation
841   monitor in Beijing, China, Atmospheric Chemistry and Physics, 18, 8469–8489, https://doi.org/10.5194/acp-18-8469-2018,
842   2018.

843   Sun, Y.-L., Zhang, Q., Schwab, J. J., Demerjian, K. L., Chen, W.-N., Bae, M.-S., Hung, H.-M., Hogrefe, O., Frank, B.,
844   Rattigan, O. V., and Lin, Y.-C.: Characterization of the sources and processes of organic and inorganic aerosols in New York
845   city with a high-resolution time-of-flight aerosol mass apectrometer, Atmospheric Chemistry and Physics, 11, 1581–1602,
846   https://doi.org/10.5194/acp-11-1581-2011, 2011.

847   Takegawa, N., Miyakawa, T., Kawamura, K., and Kondo, Y.: Contribution of Selected Dicarboxylic and ω-Oxocarboxylic
848   Acids in Ambient Aerosol to the m/z 44 Signal of an Aerodyne Aerosol Mass Spectrometer, Aerosol Science and
849   Technology, 41, 418–437, https://doi.org/10.1080/02786820701203215, 2007.

850   Tiitta, P., Vakkari, V., Croteau, P., Beukes, J. P., van Zyl, P. G., Josipovic, M., Venter, A. D., Jaars, K., Pienaar, J. J., Ng, N.
851   L., Canagaratna, M. R., Jayne, J. T., Kerminen, V.-M., Kokkola, H., Kulmala, M., Laaksonen, A., Worsnop, D. R., and
852   Laakso, L.: Chemical composition, main sources and temporal variability of PM_1 aerosols in southern African grassland,
853   Atmospheric Chemistry and Physics, 14, 1909–1927, https://doi.org/10.5194/acp-14-1909-2014, 2014.

854   Ulbrich, I. M., Canagaratna, M. R., Zhang, Q., Worsnop, D. R., and Jimenez, J. L.: Interpretation of organic components
855   from Positive Matrix Factorization of aerosol mass spectrometric data, Atmospheric Chemistry and Physics, 9, 2891–2918,
856   https://doi.org/10.5194/acp-9-2891-2009, 2009.

857   Wang, X., Williams, B. J., Wang, X., Tang, Y., Huang, Y., Kong, L., Yang, X., and Biswas, P.: Characterization of organic
858   aerosol produced during pulverized coal combustion in a drop tube furnace, Atmospheric Chemistry and Physics, 13, 10919–
859   10932, https://doi.org/10.5194/acp-13-10919-2013, 2013.

860   Weimer, S., Alfarra, M. R., Schreiber, D., Mohr, M., Prévôt, A. S. H., and Baltensperger, U.: Organic aerosol mass spectral
861   signatures from wood-burning emissions: Influence of burning conditions and wood type, Journal of Geophysical Research:
862   Atmospheres, 113, https://doi.org/10.1029/2007JD009309, 2008.

Xu, J., Zhang, Q., Chen, M., Ge, X., Ren, J., and Qin, D.: Chemical composition, sources, and processes of urban aerosols during summertime in northwest China: insights from high-resolution aerosol mass spectrometry, Atmospheric Chemistry and Physics, 14, 12593–12611, https://doi.org/10.5194/acp-14-12593-2014, 2014.

Xu, L., Suresh, S., Guo, H., Weber, R. J., and Ng, N. L.: Aerosol characterization over the southeastern United States using high-resolution aerosol mass spectrometry: spatial and seasonal variation of aerosol composition and sources with a focus on organic nitrates, Atmospheric Chemistry and Physics, 15, 7307–7336, https://doi.org/10.5194/acp-15-7307-2015, 2015.

Young, D. E., Kim, H., Parworth, C., Zhou, S., Zhang, X., Cappa, C. D., Seco, R., Kim, S., and Zhang, Q.: Influences of emission sources and meteorology on aerosol chemistry in a polluted urban environment: results from DISCOVER-AQ California, Atmospheric Chemistry and Physics, 16, 5427–5451, https://doi.org/10.5194/acp-16-5427-2016, 2016.

Zhang, Q., Alfarra, M. R., Worsnop, D. R., Allan, J. D., Coe, H., Canagaratna, M. R., and Jimenez, J. L.: Deconvolution and Quantification of Hydrocarbon-like and Oxygenated Organic Aerosols Based on Aerosol Mass Spectrometry, Environ. Sci. Technol., 39, 4938–4952, https://doi.org/10.1021/es048568l, 2005.

Zhang, Q., Jimenez, J. L., Canagaratna, M. R., Ulbrich, I. M., Ng, N. L., Worsnop, D. R., and Sun, Y.: Understanding atmospheric organic aerosols via factor analysis of aerosol mass spectrometry: a review, Anal Bioanal Chem, 401, 3045–3067, https://doi.org/10.1007/s00216-011-5355-y, 2011.

Aerosol Mass Spectrometry (AMS) Global Database: https://sites.google.com/site/amsglobaldatabase/urban-down-wind/montseny-spain, last access: 23 December 2022.

Zhang, Y., Du, W., Wang, Y., Wang, Q., Wang, H., Zheng, H., Zhang, F., Shi, H., Bian, Y., Han, Y., Fu, P., Canonaco, F., Prévôt, A. S. H., Zhu, T., Wang, P., Li, Z., and Sun, Y.: Aerosol chemistry and particle growth events at an urban downwind site in North China Plain, Atmospheric Chemistry and Physics, 18, 14637–14651, https://doi.org/10.5194/acp-18-14637-2018, 2018.

Zhao, Q., Huo, J., Yang, X., Fu, Q., Duan, Y., Liu, Y., Lin, Y., and Zhang, Q.: Chemical characterization and source identification of submicron aerosols from a year-long real-time observation at a rural site of Shanghai using an Aerosol Chemical Speciation Monitor, Atmospheric Research, 246, 105154, https://doi.org/10.1016/j.atmosres.2020.105154, 2020.

Zorn, S. R., Drewnick, F., Schott, M., Hoffmann, T., and Borrmann, S.: Characterization of the South Atlantic marine boundary layer aerosol using an aerodyne aerosol mass spectrometer, Atmospheric Chemistry and Physics, 8, 4711–4728, https://doi.org/10.5194/acp-8-4711-2008, 2008.